

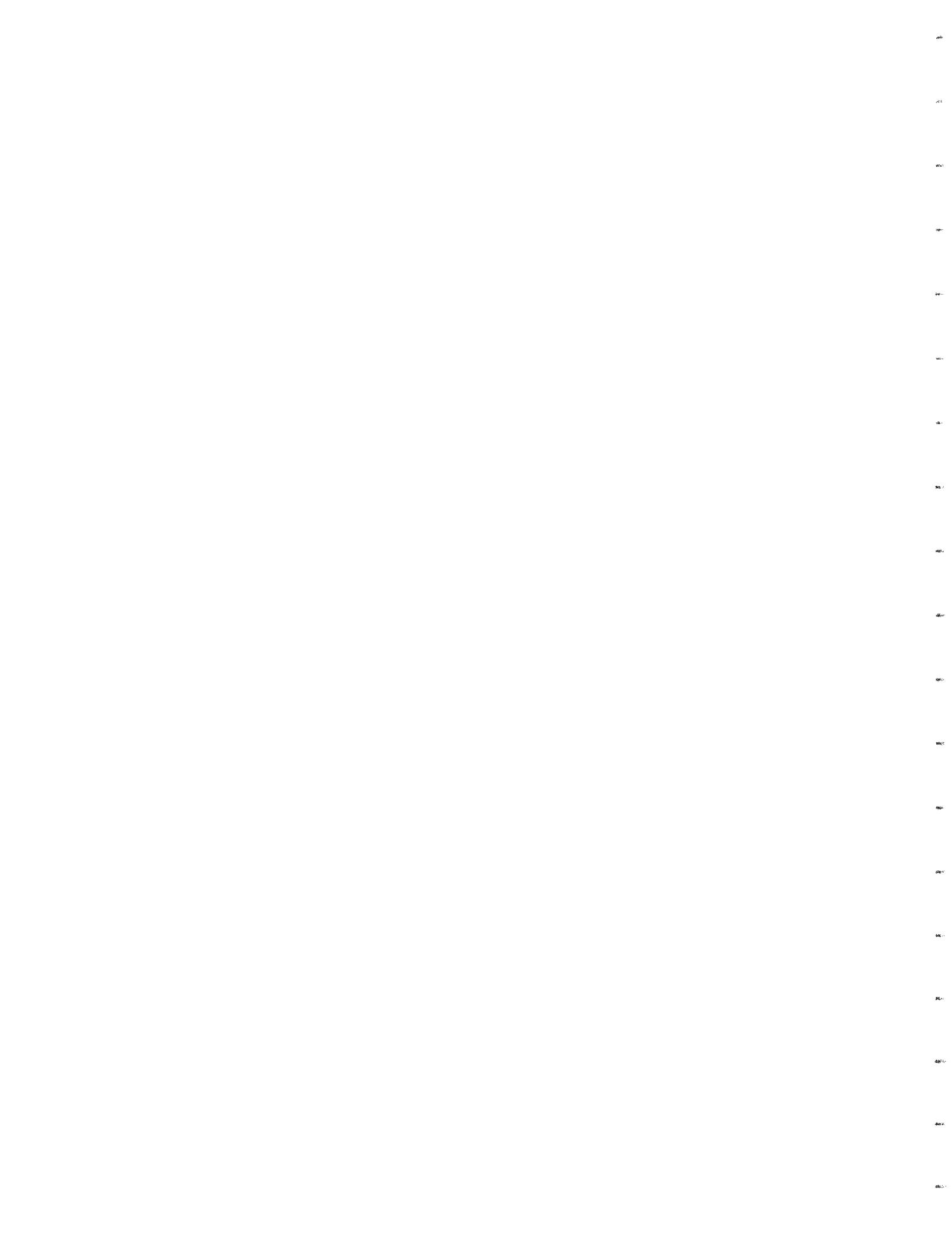
FEASIBILITY OF FUEL SWITCHING
IN BOSTON

David P. Hoult
William T. Kranz

Report No. MIT-EL 74-001
February 1974

ENERGY LABORATORY

The Energy Laboratory was established by the Massachusetts Institute of Technology as a Special Laboratory of the Institute for research on the complex societal and technological problems of the supply, demand and consumption of energy. Its full-time staff assists in focusing the diverse research at the Institute to permit undertaking of long-term interdisciplinary projects of considerable magnitude. For any specific program, the relative roles of the Energy Laboratory, other special laboratories, academic departments and laboratories depend upon the technologies and issues involved. Because close coupling with the normal academic teaching and research activities of the Institute is an important feature of the Energy Laboratory, its principal activities are conducted on the Institute's Cambridge Campus.





Energy Laboratory
Massachusetts Institute of Technology
Cambridge, Massachusetts 02139
(617) 253-3400
Room 26-167

March 29, 1974

Dr. Jerome B. Wiesner
President
Massachusetts Institute of Technology
Cambridge, Massachusetts

Dear Dr. Wiesner:

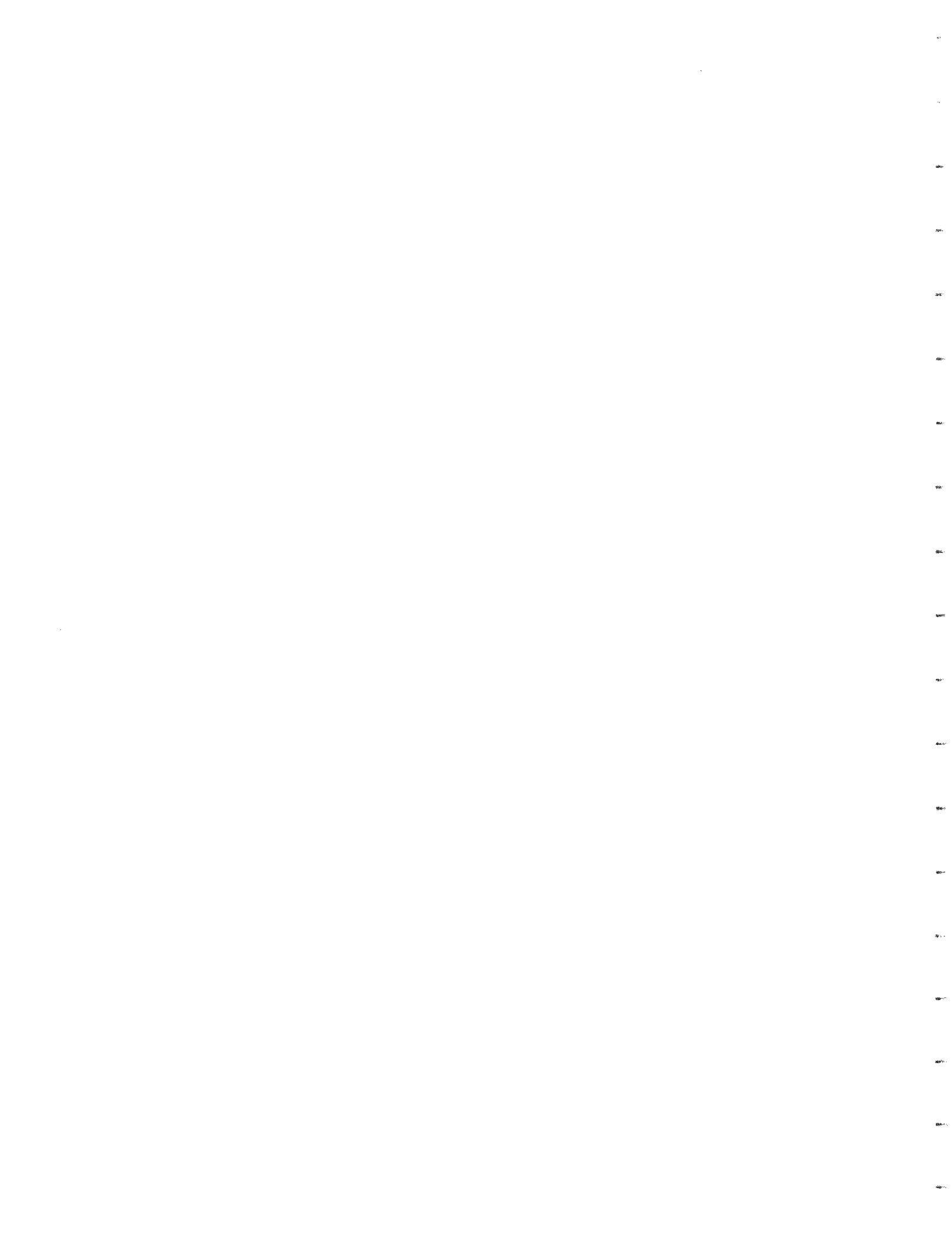
By this letter, I wish to submit to you our study "Feasibility of Fuel Switching in Boston". This study presents a theory which describes why fuel switching may be feasible in Boston. The theory contains a number of ideas which are new and relatively untried. Perhaps the most important is the concept of what defines a large source, as this issue is particularly thorny from a regulatory point of view.

The results of the theory are compared with observations of SO_2 levels in Boston. These comparisons indicate the theory is consistent with available data, and support the basic conclusion of our study, that large sources can burn high sulfur fuels during nighttime while meeting the EPA standards.

The comparison with field data is not conclusive, however, because of the large amount of scatter intrinsic in the data. Furthermore, our feasibility study deals only with the turbulent dispersion of pollutants. The simple results gotten offer the potential of a simple regulatory system which would allow large sources to burn high sulfur fuel.

But other, important, aspects of feasibility have not been considered. A proof of technical feasibility requires the design and reliability analysis of an explicit supplementary control system (S.C.S.) which is consistent (as much as possible) with the current EPA position on fuel switching for isolated sources. The analysis would involve a time of day-weather dependent study with explicit modeling of both large and small sources.

Also, we feel that an implementation program should include a better field test of our theory, and a comparison with other, older, semiempirical results, which have been used in the past as justification for fuel switching schemes.



Dr. Jerome B. Wiesner

March 29, 1974

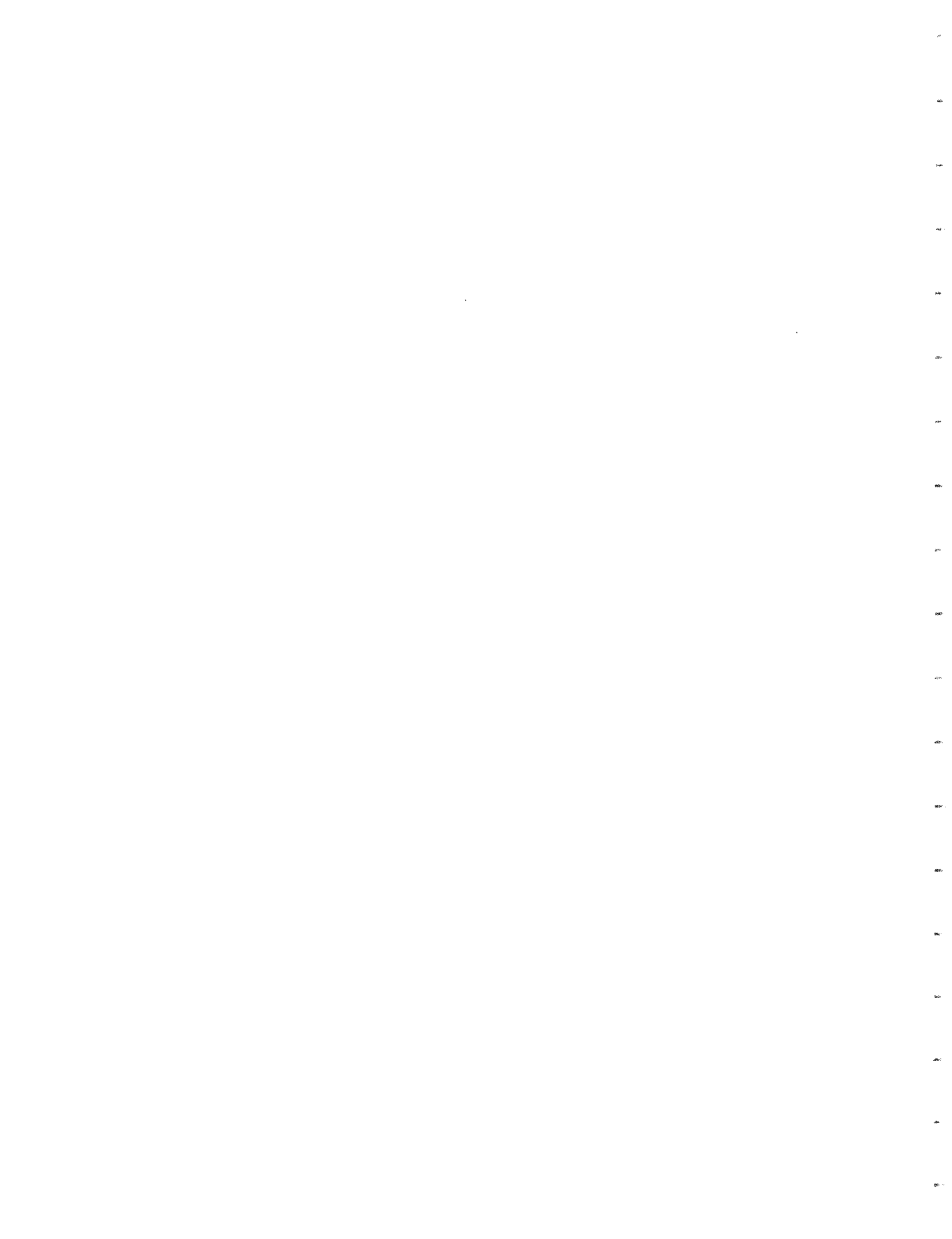
We feel that a lot more work will be required to implement a fuel switching program for Boston. Our results should help this process by suggesting simple regulatory rules.

Sincerely yours,

A handwritten signature in black ink, appearing to read "David P. Houlton". The signature is written in a cursive, flowing style.

David P. Houlton
Professor, Mechanical Engineering

DPH:ar



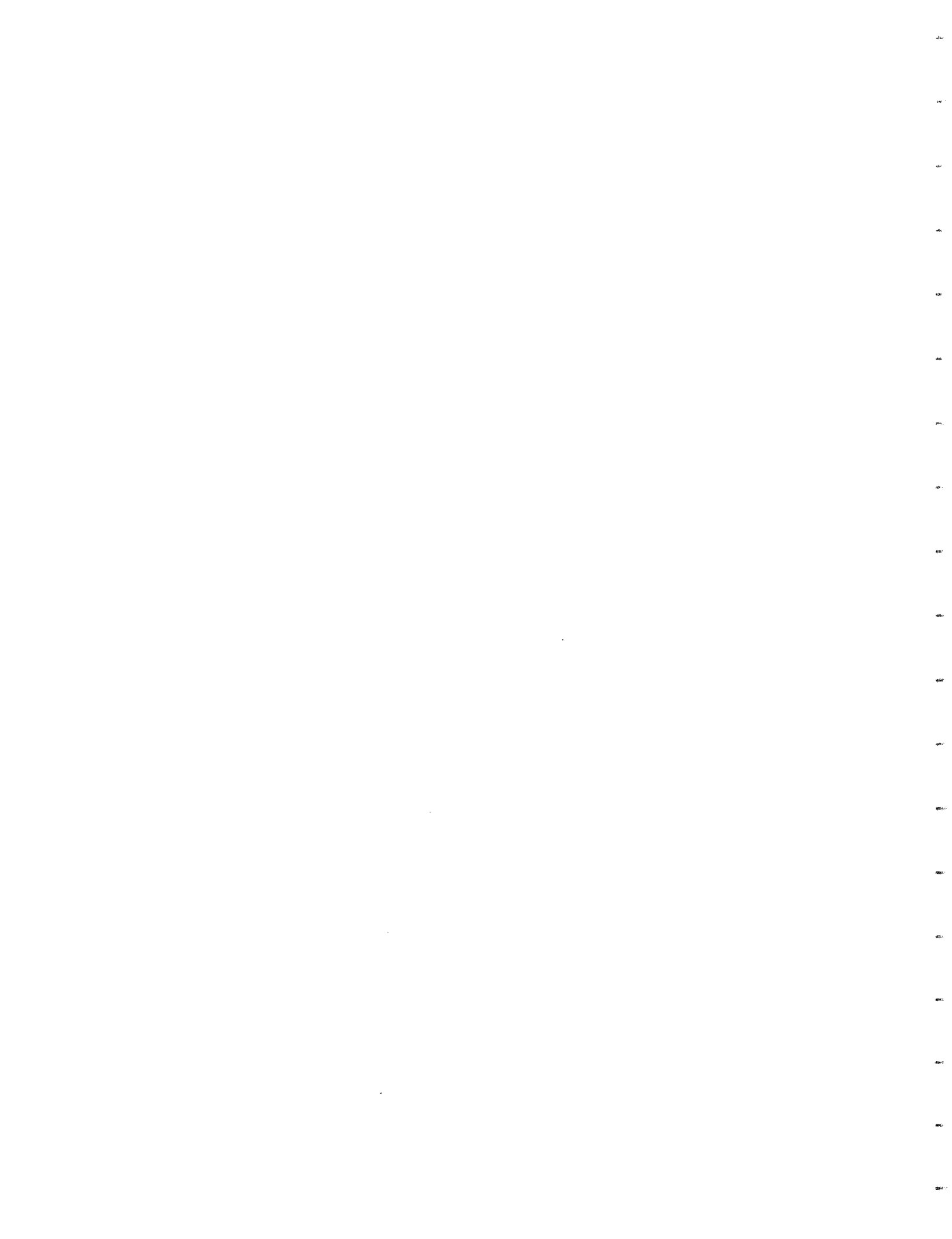
FEASIBILITY OF FUEL SWITCHING IN BOSTON*

by

David P. Hoult and William T. Kranz
Massachusetts Institute of Technology

February 28, 1974

*This research was supported by the Sloan Basic Research Fund, M.I.T.



ABSTRACT

This report develops a simple physical model that predicts that the nighttime dispersion of SO_2 from the largest sources in Boston is different than the dispersion of SO_2 from small, low level sources. Diurnal variations in SO_2 levels measured in Boston over the last seven years are analyzed in the light of this theory. The comparison between theory and observation is favorable. A simple, unambiguous, criteria for defining a large source is developed. The results are used to predict the fraction of the time large sources could burn high sulfur fuels while still meeting the state standards for sulfur dioxide.

Contents

List of Tables.....2

List of Figures.....3

Nomenclature.....4

Part I

Introduction.....6

The Model.....9

Part II

Solar Radiation.....17

Lapse Rate.....18

Wind.....18

Atmospheric Energy Budget.....20

Monin-Obukhov Length.....23

Daytime Mixing Depth.....24

Plume Rise During the Day.....27

Nighttime Mixing Depth.....28

Plume Rise During the Night.....31

Source Inventory.....32

Line Source Model.....35

Observed Air Quality.....36

Estimation of Source Strength.....37

Seasonal Concentrations.....41

Twenty Four Hour Concentrations.....43

One Hour Concentrations.....46

Fuel Switching to Meet the Standards.....50

References.....63

List of Tables

	Page
1. Monthly Solar Heat Flux, I_0	17
2. Wind Speed and Direction at Logan Airport	19
3. Heat Flux, at Ground Level, q	23
4. Monin-Obukhov Length, L^*	24
5. Daytime Mixing Depth	26
6. Nighttime Mixing Depth	30
7. Large Sources in Area Modeled	34
8. Observed Concentrations in Area Modeled	37
9. Tons SO_2 Emitted Per Year in Area Modeled	38
10. Annual Line Source Strength, Γ	39
11. Observed Monthly Mean Daytime, Nighttime and 24 Hour Average Concentrations	40
12. Seasonal Estimates of L , V , and Γ	41
13. Estimates of L , V , and Γ Which Produce 24 Hour Maximum Concentrations	42
14. Estimated 24 Hour Maximum Concentrations if Large Sources Burn 2% Sulfur Fuel	45
15. Estimates of L , and V Which Produce One Hour Maximum Concentrations	48
16. Highest Ground Level Contributions From Large Sources	49
17. Predicted One Hour Concentrations if Large Sources Burn 2% Sulfur Fuel	50
18. Summary of Predicted Concentrations if Large Sources Burn 2% Sulfur Fuel	51

List of Figures

1.	Daily Solar Heat Flux in January	54
2.	Daily Solar Heat Flux in June	54
3.	Annual Lapse Rate	55
4.	Mixing Depth at 7:00 A.M.	55
5.	Convective Mixing Depth for Winter Months at Noon	56
6.	Convective Mixing Depth for Summer Months at Noon	56
7.	Wind Speed at Logan Airport	57
8.	Point Source Size Distribution	57
9.	Section of Core Area Modeled	58
10.	Heat from Combustion vs Population	59
11.	Annual and Seasonal Daytime Concentrations	60
12.	Annual and Seasonal Nighttime Concentrations	61
13.	Seasonal 24 Hour Maximum Concentrations	62
14.	Seasonal 1 Hour Maximum Concentrations	62

Nomenclature

Abbreviations

CFM Cubic feet per minute

$^{\circ}\text{C}$ Degrees centigrade

m Meters

PPM Parts per million

SO_2 Sulfur dioxide

Symbols

b Plume radius (meters)

b_i Radius of stack exit (meters)

C Concentration (SO_2 in PPM)

C_i Ground level concentration produced by an individual point source in the absence of any other sources (PPM)

F_o Buoyancy flux $\frac{u_i b_i^2 \Delta T}{\pi \rho_o C_p T}$ (meters⁴/sec³)

C_p Specific heat of air at constant pressure ($^{\circ}\text{C}/\text{gram}$)

g Gravitational constant (9.8 meters/sec²)

h_e Effective stack height (meters)

h_s Stack height (meters)

I_o Daily solar heat flux received at ground level (cal/m²)

k Von Karman's constant (dimensionless)

K Conversion constant for SO_2 ($350 \frac{\text{PPM}}{\text{gram/m}^3}$)

L_b Buoyancy length scale (meters)

L Mixing depth (meters)

L^*	Monin-Obukhov length scale (meters)
q	Heat flux into the atmosphere at ground level ($\text{cal/m}^2\text{sec.}$)
Q_R	Solar heat flux received at ground level ($\text{cal/m}^2\text{sec.}$)
S	Downwind length dimension of city where heat flux, q , is positive (meters)
t	time (seconds)
t_d	time between sunrise and sunset (seconds)
T	Ambient temperature (degrees Kelvin)
U_i	Stack exit velocity (meters/sec.)
V	Wind speed (meters/sec.)
V^*	Friction velocity (meters/sec.)
x	Downwind distance (meters)
z	Vertical distance (meters)
z'	Vertical distance above stack exit (meters)
z'_{\max}	Total plume rise above stack Eq. 7 (meters)
β	Transverse entrainment parameter 0.6 (dimensionless)
Γ_i	Pollutant flux from an individual point source (grams/sec.)
Γ_L	Annual line source strength produced by large sources (grams/m sec.)
Γ_s	Annual line source strength produced by small sources (grams/m sec.)
Γ_t	Annual line source strength produced by all sources (grams/m sec.)
Δh	Plume rise when lapse rate is constant in the region of plume rise, Eqs. 13 and 16 (meters)
ΔT	Difference between stack exit temperature and ambient temperature (degrees) (Kelvin)
θ	Potential temperature (degrees centigrade)



PART I

I. Introduction

In order to control SO_2 levels in Boston, restrictions have been placed on the sulfur contents of fuels burned in the Boston area. The concept of fuel switching is that there are certain favorable periods of time during which some sources may burn high sulfur fuel, and other, unfavorable periods during which low sulfur fuels must be burned to meet the environmental standards for SO_2 . This concept would be viable if one could show that high sulfur fuel could be burned a substantial fraction of the time while still meeting the standards.

There are a number of questions which are raised by this concept. Perhaps the most important is whether the SO_2 from all sources is dispersed in the same way. It has been suggested (Refs. 1,2) that the pollution from large sources is dispersed in a manner different from small sources. If this is valid, then there must be some rational way to decide which is a large source and which is a small source. Then, again, what are the favorable (unfavorable) periods of time? And what role does the size and geometry of the city play in such a concept?

It is the task of this report to bring a number of technical ideas to bear on these questions. First, there is an extensive literature on the aerodynamics of plumes from individual chimneys (Ref. 3). This literature consists of a theory (Ref. 4) correlations of field observations (Ref. 5) and laboratory experiments (Ref. 6). In addition, there is a theory of how

large, buoyant plumes mix down to ground level. This theory has been compared with field observations (Ref. 7). But, of course, these plumes are ejected into a complex atmospheric flow.

There is a fairly well developed understanding of this flow. The Monin-Obukhov theory (Ref. 3) describes the lowest 30 meters of this flow. It has been compared with both laboratory experiments (Ref. 9) and field observations (Ref. 10). The additional heat flux from cities causes them to be hotter than their suburbs, especially at night. The changes in the air flow over the city due to this heating effect have been studied (Refs. 11-16). Finally, there is a well developed theory of the case when convective motions caused by strong solar heating dominate the mechanically generated turbulence (Ref. 7). These past researches are the tools which we may apply to study fuel switching.

Then, there is a substantial body of data which we may profitably study to understand this complex problem. First, there are weather records of various kinds for the city of Boston. Second, there is radiosonde data, which give temperature variations with altitude (Ref. 17). There are the air pollution records of SO_2 levels (Ref. 18). There is an inventory of the major air pollution sources in the area (Refs. 19,20). And finally, there is an historical record of the changing regulations of sulfur content in fuels (Ref. 21).

The purpose of this report is first, to develop a simple conceptual model to show that the dispersion from large sources is different in daytime and nighttime. A theory which allows one to calculate, for a given city,

which are large and which are small sources is presented. Second, this theory is used to correlate the Boston air pollution data of the past seven years. Although the observations over these years turn out to be consistent with the theory, due to the inherent scatter in the data and the many factors which influence the data, one cannot prove conclusively that the theory is correct. But one can use the correlations of the data generated by the theory to estimate the fraction of the time large sources can burn high sulfur fuel, and hence determine the feasibility of fuel switching.

This report is divided into two parts. This part, Part I, describes the theoretical model and the results of correlating the air pollution data. Part II describes the complex details of the Boston weather, the source inventory, the manner in which the calculations were carried out, and in short, all the details necessary to support Part I.

The Model

Consider first the daytime city. At sunrise, the solar heat begins to warm the city. A substantial fraction of the solar heat reaching the ground (55%) is transferred to the surrounding air by a process of turbulent heat transfer. The energy so transferred gradually destroys the stable layer of air which covers the city during nighttime. Weil and Hout (Ref. 7) show that this process produces an adiabatic layer whose height increases with time through the day. We denote the depth of this mixing layer L . The formula that Weil and Hout developed is

$$L = \left[\frac{2 \int_0^t q dt}{\frac{d\theta}{dz} \rho_o C_p} \right]^{1/2} \quad \text{Eq. (1)}$$

Using this formula, one can calculate the height of the adiabatic layer and compare the result with radiosonde data. There is good agreement (see page (26) Part II). L is typically about 850 m by early afternoon.

In this layer, the heat flux from the ground causes a convective motion which **dominates** the mechanically generated turbulence. To see this, we use the concepts developed by Monin and Obukhov (Ref. 10). They have shown that for altitudes greater than a certain height, L^* (traditionally called the Monin-Obukhov length), convective turbulence dominates mechanically produced turbulence. L^* is given by

$$L^* = \left| \frac{v_*^3 \rho C_p T}{k g q} \right| \quad \text{Eq. (2)}$$

The mixing depth varies with time according to Eq.(1). L is about 100 meters at 7:00 a.m., and increases to over 1000 meters by the end of a summer afternoon. In the winter, L is less because the solar radiation is less.

For a 11.2 knot wind (the average wind speed in Boston (page 19), L^* is about 35 meters during the day. Clearly $L \gg L^*$.

These results constitute our model of the daytime air flow over the city.

During the night, a radically different air flow is generated. Soon after sunset, the ground in rural areas is cooled by long wave radiation to the sky. The ground cools the air adjacent to it, generating a stably stratified flow. This stable air flow gets modified when it reaches the city, rather like the way a turbulent boundary layer is modified when it flows over a hot surface. These modifications depend on the turbulent heat flux from the nighttime city. We estimate this heat flux in the following way. We calculate the annual fuel consumption in the ten square kilometer core area of Boston. During nighttime, we estimate that the heat leaves the core area at approximately this annual rate. The heat loss due to long wave radiation is estimated and subtracted from the city heat flux. The result is a positive heat flux, q , into the air at night. (Page 21).

As the air flows over the city, this heat flux causes the lower levels of air flow to become well mixed. An estimate of the depth of this layer was given by Summers (Ref. 13)

$$L = \left[\frac{2qS}{\frac{d\theta}{dz} \rho_o C_p V} \right]^{1/2} \quad \text{Eq. (3)}$$

Here S is the length dimension of the core area of the city. For Boston we use 10km . As a result of the detailed discussion on page 29, the estimate of the nighttime mixing depth is 100m. The value is consistent with the observed adiabatic layer depth obtained from early morning radio-sonde data (page 30).

During the nighttime L^* is of the order of 1000 meters, depending on the value of q . The nighttime heat flux into the air from a city is highly variable because of the seasonal variation in space heating and the effect of clouds which can reduce the long wave loss observed on clear nights by 80% (Ref. 22). For Boston it is clear that $L < L^*$ and mechanically generated turbulence dominates the diffusion process in the mixing layer during the night.

There is a very significant feature of this nighttime flow: for very large cities, such as New York, the nighttime heat flux into the air can be the same as the daytime heat flux. If the city is large enough $L > L^*$ and convective mixing occurs during the night as well as the day. This undoubtedly happens on some nights in New York causing the large source criteria to be much more stringent for New York (see page 31 and Table 4).

Now let us examine the aerodynamics of a chimney plume during the daytime in Boston. From plume aerodynamic theory, it is well documented (Ref. 5) that the plume rise in a neutral atmosphere varies with distance downwind, x , as

$$z' \sim l_b^{1/3} x^{2/3} \qquad \text{Eq. (4)}$$

In Eq.(4), l_b is the buoyancy length scale,

$$l_b = F_o / V^3 \quad \text{Eq. (5)}$$

Eq.(4) is based on the idea that the buoyancy flux in a plume is conserved in a neutral atmosphere. A plume would rise forever if its buoyancy were preserved.

When a plume encounters a layer of stable air, the buoyancy decreases; when it reaches zero, the plume levels off. Equations are available to calculate this altitude, Eq.(16).

During the daytime, however, the rise, Eq.(4) occurs in a region $z < L$, where there is a strong convective mixing process occurring ($L > L^*$). A feature of this convective process is the existence of alternate currents of hot air (rising) and cold air (descending) in the mixing layer. Weil and Hault (Ref. 7) show that such a pattern of positive and negative buoyancy fluxes causes the orderly rise of the plume to be broken up, and parts of the plume to be mixed down to ground level.

Detailed calculations (page 27) show that within a few hours of sunrise $L > L^*$ and the plumes from even the largest sources in Boston will be dispersed by this process.

The dispersion generated by this process tends to uniformly mix the pollutants throughout L . To compare this conclusion with observations, the SO_2 sources in the 10 square Km center of Boston were totalled. The sources were considered to be located on a hypothetical line, 10 Km long, normal to the wind speed V . In this way a line source strength Γ was estimated, for both summer and winter conditions (see page 38). The

concentration of SO_2 then is given by (page 35)

$$C = K \frac{\Gamma}{VL}$$

Due to the changes in source strength Γ arising from changing regulations, one can calculate a variety of concentrations. When these concentrations are compared with observations the deduced values are in good agreement with the observations, (page 41 and Figs. (11-14)). There is also good agreement between the observed L and the L determined by Eq.(1), (page 26).

Turning to the nighttime behavior of plumes, we must consider the plume rise in the neutrally stable mixing layer ($L < L^*$), followed by rise and levelling off in the stable region above L . Let Δh be the plume rise in this latter region. Δh may be estimated by using the average lapse rate above the stable layer, if the buoyancy flux of the source is given, (page 31). According to plume aerodynamic theory, (Ref. 6) the width of the plume when it levels off is

$$b = \beta z'_{\max} \quad \text{Eq. (6)}$$

where z'_{\max} is the total rise above stack height:

$$z'_{\max} = (L - h_g) + \Delta h \quad \text{Eq. (7)}$$

The height of the plume centerline, when the plume is level, is $(h_g + z'_{\max})$.

It is convenient to distinguish two different outcomes of this plume rise process. For very large sources, the plume will penetrate the stable layer to such an altitude that the lower edge of the plume will be higher than L . This requirement, that the plume be completely trapped in the

stable layer, amounts to

$$h_s + z'_{\max} (1 - \beta) > L \quad \text{Eq. (8)}$$

For such plumes, the dispersion process is essentially zero, according to plume aerodynamics. The plume will drift downwind until daylight before being mixed down to ground level. Actually, there will be a slow dispersion process due to a small, non-zero eddy diffusivity in the stable flow. However, many observations of plumes in stable air suggest that this dispersion is not adequate to mix the plume over any appreciable extent, (Ref. 7).

For very small sources, the plume rise in the stable layer above L is very small. In this limit, the plume centerline levels off at L , so that:

$$\Delta h = 0 \quad \text{Eq. (9)}$$

Then the plume extends βL into the stable region and βL into the mixing layer. Under such circumstances, one-half of the plume will be mixed down to ground level due to mechanically generated turbulence.

It is appropriate to categorize as large sources all those plumes which obey Eq.(8).

These considerations serve to define the large and small source inventory of a city. One half of the effluent from small sources is mixed in the region $0 < z < L$.

Excepting those instances when the plume from a large source is drawn into the elevated air intakes of large buildings, and provided the wind

speed is high enough to carry the large source nighttime emissions downwind of the city before dawn, one can argue that large sources are not a source of local city pollution at night. The mean wind speed in Boston, 11.2 knots, is sufficient for the latter requirement to be met.

Calculations following Tsang's (Ref. 23) analysis of field data on plumes show that when a plume has been convected downwind some 10Km or more, the concentration of pollutants in it is so low as not to violate the ambient air quality standards when it is mixed down to ground level at dawn.

This behavior of large sources is the basic reason that it is sensible to allow large sources to burn high sulfur fuel at night.

Using this model, we have constructed correlations of the observed SO₂ levels in the Boston area. The determination of the source strengths were made by using the source inventory, adjusting the source strength to take account of the changes in fuel regulations over the years, and then correlating the concentrations. In all cases, the concentrations (mixing depths) were in good agreement with those determined by the model. Correlations of the hourly, 24 hour and yearly average were made, (pages 41 to 49). The results are shown in Figs.(11-14).

These correlations can be used to determine the fraction of the time the large sources could switch to high sulfur fuel. The standards used by the Mass. Dept. of Public Health are assumed to represent the lower limit for air quality. They are as follows: 1 hour max. = 0.28 ppm; 24 hour max = 0.105 ppm, yearly average = 0.025 ppm. In order to add an additional safety factor, the fraction of time large sources could be high sulfur fuel is based on the assumption that the predicted air quality must remain 25% below maximum

acceptable levels listed above.

In order to determine the restrictions imposed by the maximum allowable hourly concentrations for sulfur dioxide it was necessary to estimate the peak background concentrations in Boston. The contribution from individual sources was calculated and added to the background concentration to determine the local one hour maximum concentration, (page 46). The area sources are individually so small that they are expected to produce no significant effect on the hourly maximum concentrations. This is not the case for the hourly contributions from the individual large point sources during the daytime. These contributions are frequently larger than the background concentration, even when the large sources are burning low sulfur fuel.

Our calculations show that the hourly and daily average concentrations are more difficult to meet than the annual average. The large scope of the study recently released by the Harvard School of Public Health, (Ref. 1) made it impossible for the report to deal with microscale air quality, similarly the shortest sampling period analyzed is 24 hours. Our findings indicate that the local hourly concentrations occurring below individual plumes from large sources must be carefully examined before these sources are allowed to burn high sulfur fuel. Although the daily (background) concentrations are low during the summer the hourly contributions from large sources are highest during this period.

In the winter the large sources in the core area can burn 2% sulfur fuel

80% of the time, provided they switch to 0.5% fuel at appropriate times. In the summertime, the large sources in the core area can burn 2% sulfur fuel for about 55% of the time, and 0.5% for the remainder, (page 53). Fuel switching done for these fractions of the time will produce hourly, daily, and annual average concentrations below or equal to the Mass. Dept. of Public Health standards.

Part II

Solar Radiation

Solar radiation measurements are valuable in determining the convective mixing depth and the velocity of the convective turbulence cells. Measurements of the total daily solar heat flux reaching the ground, I_0 , were obtained for the Boston area between 1971 and 1972, (Ref. 24). Table 1 presents: a) the average daily heat flux by month and b) the maximum possible daily heat flux. Both are measured in cal./cm^2

Table 1

	Jan.	Feb.	March	April	May	June	July	Aug.	Sept.	Oct.	Nov.	Dec.
a)	135	150	261	344	390	530	415	478	317	215	150	100
b)	340	480	650	900	1000	1040	1000	950	730	540	380	300

The cumulative frequency distribution for the daily solar heat flux in January (winter months) and June (summer months) is presented in Figs. (1 and 2).

Lapse Rate

The lapse rate, vertical temperature gradient, is a measure of atmospheric stability. It is used to estimate both plume rise and the growth of the convective mixing depth. In the following discussion the lapse rate will be measured in terms of potential temperature, $\frac{d\theta}{dz}$.

An adiabatic lapse rate is produced by a heat flux at ground level caused either by solar heating or heat rejection from an urban area. The neutral buoyancy associated with an adiabatic lapse rate, $\frac{d\theta}{dz} = 0$, allows uniform mixing throughout the region. The depth of the adiabatic layer above the ground is called the mixing depth because pollutants are uniformly mixed throughout this region if they reach equilibrium in it.

The normal state of the lower atmosphere is stable. The average annual lapse rate near the ground in the Northern Hemisphere is $\frac{d\theta}{dz} = 3.5 \times 10^{-3} \text{ }^{\circ}\text{C/m}$ (Ref. 22). Examination of local radiosonde data (Ref. 17) suggests that the average lapse rate above the mixing layer during the day is $\frac{d\theta}{dz} = 5 \times 10^{-3} \text{ }^{\circ}\text{C/m}$. Vertical mixing is inhibited in this stable region of the atmosphere and pollutants which reach equilibrium in the stable region tend to remain at their equilibrium height. The observed frequency distribution for the morning lapse rate above the mixing layer is shown in Fig. 3.

Wind

Table 2 presents the annual average wind data for Logan International Airport, (Ref. 25). Annually the prevailing wind direction is from the west and the average wind speed is about 11 knots (5.75 meters/sec.). In the winter the prevailing wind direction is from the northwest with an

Table 2 (Ref. 25)

Percentage Frequency of Wind Direction 1945-65

Wind Direction	N	NNE	NE	ENE	E	ESE	SE	SSE	S	SSW	SW	WSW	W	WNW	NW	NNW
Annual	4.7	3.8	4.1	4.0	4.4	4.7	3.7	3.1	4.4	7.5	10.9	7.3	8.1	11.4	10.1	7.1
Jan. (Winter)	7.2	3.4	2.9	1.9	1.6	1.5	1.9	2.5	3.3	5.0	8.6	7.6	10.1	15.1	15.8	15.9
June (Summer)	3.1	3.1	4.0	4.8	5.7	6.2	4.5	3.5	5.0	10.6	15.3	8.0	7.0	8.1	6.3	4.1

Percentage Frequency of Wind Speed 1945-65

Wind Speed (Knots)	1-3	4-6	7-10	11-16	17-21	22-27	28-33	34-40	Mean
Annual	3.4	13.0	34.2	9.7	3.5	.7	.1	.0	11.2
Jan. (Winter)	3.1	10.9	27.6	36.5	14.1	5.6	1.4	.2	12.4
June (Summer)	3.6	14.8	37.7	35.6	6.3	1.1	.1	.0	9.6

average speed of 12 knots (6.4 meters/sec.). In the summer the prevailing wind direction is from the southwest with an average speed of 10 knots (5.2 meters/sec.). Fig. (7) shows the cumulative frequency distribution for the annual wind speed in meters/sec. and ft/sec.

Atmospheric Energy Budget

The depth of the mixing layer, Eqs. (1 and 3), and the Monin-Obukhov length, L^* Eq.(2), are both dependent on the heat flux, q , from the ground to the atmosphere. In an urban area the heat sources are solar radiation and combustion within the city. Heat is lost by black body radiation from the earth's surface back into space.

Black body radiation (long wave) at the earth's surface radiates approximately $0.6 \text{ cal/cm}^2 \text{ min}$. Most of this long wave radiation is absorbed by the constituents in the atmosphere, principally water vapor, and reradiated back to the earth's surface. The average net loss due to long wave radiation at this latitude ($40^\circ - 50^\circ \text{ N}$) is $0.12 \text{ cal/cm}^2 \text{ min}$. (Ref. 26). More water vapor in the atmosphere (cloudy skies) decreases the net long wave loss. The variation between cloudy and clear skies can be as much as 80% (Ref. 26).

By regression analysis of world wide data, Davies (Ref. 27) estimated the average daily heat flux into the atmosphere is 55% of the solar energy received at ground level. The remaining 45% of the solar energy is lost due to long wave radiation or stored in the ground. The heat flux into the atmosphere is the sum of the latent heat of evaporation and the sensible heat flux q . It is assumed that during the day $q = .55 Q_r$. This gives

a reasonable estimate, but neglects both the latent heat of evaporation and the heat of combustion in urban areas, (Table 3).

The intensity of the solar radiation, Q_r , varies sinusoidally during the day, reaching a peak at solar noon. The total heat flux during the day is I_0 . If $t = 0$ at sunrise and $t = t_d$ at sunset, the following approximation adequately describes the variation of the solar heat flux with time.

$$Q_r = \frac{\pi I_0}{2t_d} \sin\left(\frac{\pi t}{t_d}\right) \quad \text{Eq.(10)}$$

The maximum intensity reached at solar noon ($t = t_d/2$) is $\frac{\pi I_0}{2t_d}$.

When $t = t_d/6$ (between 9:00 and 10:00 A.M.) the solar heat flux reaches half of its maximum value. Table 3 lists the estimated heat flux to the atmosphere, $q = .55 Q_r$, at solar noon.

At night, if there are no major heat sources (cities), the heat loss due to long wave radiation cools the earth's surface. The thermal energy stored in the atmosphere is transferred back to the earth's surface and radiated into space. Observations indicate that the average nighttime sensible heat flux, q , is between $-.05$ and $-.07 \text{ cal/cm}^2 \text{ min.}$ (Refs. 10,26,28). During the night about half the long wave heat loss is supplied by the atmosphere, the rest comes from the heat stored in the ground during the day.

The only estimate of the heat flux from a city currently available is based on the annual fuel consumption. This neglects the high thermal storage capability of urban areas (Ref. 29). Similarly it does not account

for diurnal or seasonal changes in fuel consumption.

It is assumed that the city heat flux reduces the amount of heat lost by the atmosphere during the night. When the average heat flux from a city is greater than $0.06 \text{ cal/cm}^2 \text{ min}$, the nighttime heat flux into the atmosphere, q , will be positive, (Table 3).

Fig.(10) indicates that the heat flux due to combustion in an urban area (Refs. 19,30) is proportional to the population density. The broken line indicates that fuel use per person in the United States (Ref. 31) follows the same trend. When the city heat flux is greater than $0.06 \text{ cal/cm}^2 \text{ min}$ the population density is between 5-10 thousand people per square mile, therefore a positive nighttime heat flux is expected for regions with greater population densities.

The size of the urban area is important because in general both fuel use and population density increase toward the center of the city. When fuel combustion figures for metropolitan Boston are examined the average nighttime heat flux is negative. However, in the small section at the core of the city the heat flux is positive (Fig. 10). A similar trend is expected for New York City, although the average nighttime heat flux is positive for the entire metropolitan area it should reach at peak in Manhattan.

Table 3
(In cal/cm²min.)

	Winter	Summer	Annual Average
Solar heat flux at noon	0.50	0.75	0.65
Estimated daytime q	0.27	0.41	0.36
	Boston Metropolitan Area	Boston Core Area	New York Metropolitan Area
Average heat of combustion	.017	.073	.105
Estimated nighttime q	-.043	.013	.045

Monin-Obukhov Length

The Monin-Obukhov length scale was determined from dimensionless analysis of the atmospheric boundary layer. At heights less than L^* mechanical turbulence dominates the diffusion process. During the day L^* is small because there is strong solar heating and convective turbulence is dominant above 30 to 100 meters (depending on the heat flux). At night there is generally a negative heat flux which produces strong stability. Stability inhibits turbulence so that L^* is small when the magnitude of the heat flux, q , is large.

Aside from the heat flux, the major variable in determining the Monin-Obukhov length is the friction velocity V^* (Refs. 8,10)

$$V^* = \sqrt{\tau/\rho} \quad \text{Eq.(11)}$$

Where τ is the stress in the boundary layer. Monin-Obukhov estimate that with unstable conditions V^* equals 8% of the wind speed V measured at an altitude of 8 meters (Ref. 10). Using the average wind speed in Boston, V^* is 0.46 meters/sec. Substitution of this value for V^* into Eq.(2) allows a rough estimate of L^* for the different heat fluxes observed in Boston. Since the wind speed in New York is about the same, the same friction velocity, $V^* = 0.46$, is used to estimate L^* in New York. Using the heat flux estimated previously the following average values for the Monin-Obukhov length are obtained (Table 4).

Table 4

	Daytime		Nighttime	
	Mid morning	Noon	Boston Core Area	New York Metropolitan Area
L^* (Meters)	80	40	1000	300
L (Average) From Tables 5 and 6	300	850	100	300

Daytime Mixing Depth

The mixing depth Eqs.(1 and 3) result from considerations of the amount of energy required to produce an adiabatic layer when the lapse rate, $\frac{d\theta}{dz}$, prior to the formation of the mixing layer is known. The sinusoidal variation in Q_r and q , defines the growth of the mixing layer throughout the day.

This model predicts that the growth of the mixing layer will be nearly linear until solar noon when it reaches 3/4 of its final height. The average mixing depth during the daylight hours is equal to the depth at solar noon. The solar heat flux and resulting convective turbulence reaches a maximum at solar noon. This causes the contribution to ground level concentrations from large sources to be highest at this time (Ref. 32). Estimates of the mixing depth at solar noon can be obtained from radiosonde measurements of the adiabatic depth or by applying Eq.(1).

Holzworth (Ref. 32) has compiled estimates of the morning and afternoon mixing depth for the United States. Radiosound data from New York, Nantucket, and Portland, Maine, were extrapolated to determine the mixing depth near Boston. Holzworth's afternoon mixing depth is assumed to be about 20% higher than the depth at solar noon.

A limited number of radiosonde ascents in Boston were examined to determine the local mixing depth. The cumulative frequency distribution obtained from these ascents is shown in Figs. (5 and 6). The summer mixing depth at solar noon is extrapolated from the 11:30 daylight savings time ascent.

At solar noon one half the total daily solar heat flux has reached the ground, therefore the integral in Eq.(1) equals, $.55 I_o/2$. The mixing depth at solar noon is:

$$L(t = \frac{t_d}{2}) = \left[\frac{.55 I_o}{\frac{d\theta}{dz} \rho_o C_p} \right]^{1/2} \quad \text{Eq.(12)}$$

The average seasonal value of L at solar noon is obtained by using the average solar heat flux (Table 1) and the average lapse rate,

$$\frac{d\theta}{dz} = 5 \times 10^{-3} \frac{^{\circ}\text{C}}{\text{m}} .$$

Table 5 lists the mixing depth at solar noon for these three different estimation techniques. There is very good agreement for the winter mixing depth. The summer mixing depth estimated from Eq.(1) is too high. This is probably due to the sea breeze, which brings air inland from the ocean. The mixing layer over the ocean is lower because more heat is absorbed by water than land masses (Refs. 26 and 33). The seasonal daytime mixing depth used in the following calculations is an average of the three estimated values.

Table 5

	Mixing Depth (Meters) at Noon		
	Winter	Summer	Annual
80% of Holzworth's afternoon depth	720	1000	920
Boston radiosonde observations (mean)	700	820	
Calculated from Eq.(1)	700	1250	
Average of above	700	1000	850

The growth rate of the mixing layer may be estimated by dividing the mixing depth at solar noon by the time elapsed since dawn, $t = t_d/2$. There are approximately eight hours of daylight in the winter and sixteen

during the summer. On the average the mixing layer grows 150 meters/hour. The average growth rate is slightly faster during the winter, presumably because less heat is lost due to evaporation and the ocean during the winter.

Plume Rise During the Day

During the day convective turbulence dominates that mixing process in the mixing layer, $L^* < L$. Plume rise in an unstable atmosphere has been described by Weil and Hault (Refs. 7 and 32)

$$\Delta h = 5.6 \frac{U_i b_i^2 T}{v} \left(\frac{g}{T}\right)^{1/3} \left(\frac{Q_r L}{\rho_o C_p}\right)^{-2/3} \quad \text{Eq.(13)}$$

Where U_i, b_i and ΔT are the stack exit parameters and T is the ambient temperature in degrees Kelvin. Eq.(13) is used to determine the effective stack height, h_e , for large sources during most of the day.

$$h_e = h_s + \Delta h \quad \text{Eq.(14)}$$

When the effective stack height is less than the mixing depth the plume is broken up and uniformly mixed throughout the mixing layer. If the effective stack height is greater than the mixing layer (possible for large sources in the early morning or late afternoon) Eq.(13) is not valid. The plume conserves buoyancy in the mixing layer and reaches equilibrium in the stable region above the mixing layer. In this case Eq.(7) must be used to calculate the plume rise.

With the annual average heat flux, the mixing layer will reach 300

meters after two hours(out of a twelve hour day). The product of $Q_r L$ at this time is large enough that the effective stack height for all sources in Boston will be below the mixing layer. It follows that all pollutants are trapped in the mixing layer within a few hours after sunrise.

Nighttime Mixing Depth

During the day the solar heat flux is relatively uniform over large areas, therefore horizontal movement of air masses over the earth's surface can be neglected when the heat flux q is calculated. At night the heat flux is negative over most of the earth's surface, however there exist small "heat islands" (urban areas) where the heat flux is positive. To estimate the mixing depth over an urban area the length of time a given parcel of air is above the city must be known as well as the heat flux.

If a control volume of air is chosen, it will move across the city at the mean wind speed, V . The heat flux is positive over a small portion of the earth's surface. The downwind dimension, S , of this region is estimated as that portion of the urban area where the population density is greater than 5000 people per square mile (page 22). The length of time that the control volume is absorbing heat from the urban area is $t = S/V$.

The nighttime heat flux from a city is assumed to be constant, so the integral in Eq.(1) can be replaced by the heat received by the control volume as it passes over the city:

$$\int_0^t q dt = q S/V \quad (\text{Eq.15})$$

If this substitution is made, Eq.(1) becomes identical with Eq.(3).

Outside the urban area radiative cooling produces a strongly stable region near the ground (ground level inversion). Hosler (Ref. 34) reports that the lapse rate in lowest 500 feet of the atmosphere in the northeastern United States is more stable than isothermal, $\frac{d\theta}{dz} > 10^{-2} \text{ }^{\circ}\text{C/m}$, almost 50% of the time at night. The average nighttime lapse rate in rural areas is assumed to be isothermal. This air is blown over the city, therefore to estimate the nighttime mixing depth an isothermal lapse rate is used in Eq.(3).

Observations of the nighttime mixing depth (heat island) with radiosonde ascents are difficult to make. The mixing depth is rarely more than two hundred meters and the radiosonde balloon is rising too fast to get accurate data points in this region. Secondly, radiosonde balloons are generally visually tracked to determine the altitude: this requires that the ascents be made during the day. Radiosonde ascents were made in Boston (Ref. 17) just after dawn for two years. The cumulative frequency distribution for the mixing depth obtained from these soundings is plotted in Fig.(4). Since the ascents were made after sunrise, the observed mixing depth is partially due to solar heating. The observed mean mixing depth is 136 meters.

The best measurements of the nighttime mixing depth have been made by helicopter flights (Refs. 14,15,16). The mixing depth has been observed over a significant period of time in New York, 300 meters (Ref. 14), and in Montreal, 100 meters (Ref. 13). Although fuel consumption information for Montreal is unavailable its area and population distribution is similar to Boston. Montreal and Boston are therefore expected to have the same mixing depth at night. The mean mixing depth obtained from the morning radiosonde

in Boston is 36 meters higher than the nighttime mixing depth in Montreal. Given the accuracy of the Boston measurement, this is very good agreement. In the remaining discussion the mean nighttime mixing depth in Boston will be assumed to be 100 meters.

The nighttime mixing depth can be predicted for Boston and New York using the average nighttime heat flux (Table 3) with Eq.(3). The predicted and observed mixing depth are listed in Table 6. In general the heat flux and population density in a city increases toward the center. It follows that the cross section of the mixing layer over a city will be hemispherical; this is supported by the observations in New York (Ref. 15). The observed depth in Table 6 is the peak of the mixing layer while the mixing depth estimated by Eq.(3) is the average cross wind depth at the down wind edge of the city. It follows that the estimated depth should be 25% lower than the observed peak. Although the mixing depths predicted in this manner are too low, the correlation which does exist indicates that the assumptions about the average nighttime heat flux are underestimated, by at most, a factor of two.

Table 6

	Boston	New York
observed L(meters)	100	300
predicted L(meters)	50	150
length of city S(meters)	10^4	2.3×10^4

Plume Rise During the Night

In most places (including Boston) the nighttime mixing depth is less than the Monin-Obukhov length, $L < L^*$. Mechanical mixing dominates the diffusion process, and Eq.(13) is not a valid description of the plume rise process ($h_e > L$ for most sources). Plumes rise through the mixing layer with no loss of buoyancy and reach equilibrium in the stable region above the mixing layer. Plume rise in the stable region is governed by Eq.(16), (Refs. 4 and 32).

$$\Delta h = 2.3 \left[\frac{U_i b_i^2 \Delta T}{v \frac{d\theta}{dz}} \right]^{1/3} \quad \text{Eq.(16)}$$

The stack exit conditions U_i, b_i , and ΔT can be used to determine plume rise in the stable region because buoyancy is conserved in the mixing layer when $L < L^*$. This Δh is used in Eqs.(7 and 17) in order to determine which sources contribute to the concentration of pollutants in the mixing layer.

In very large cities such as New York the nighttime heat flux can be large enough that $L \geq L^*$. In such cases convective mixing dominates the diffusion process during the nighttime as well as the daytime. New York is a borderline case with the current accuracy of the heat flux measurements. If Eq.(13) is applied to the nighttime mixing layer and heat flux in New York, the product of $Q_r L$ is such that the largest source in Boston would have an effective stack height below the top of the mixing layer. It is probable that the majority of sources in New York are trapped in the mixing

layer at night, especially during the winter when the heat flux from space heating is greatest (Refs. 15 and 30).

Source Inventory

Large sources are defined on page 13 as those sources for which the equilibrium position of the bottom of the plume is above the nighttime mixing depth. Pollutants emitted from such sources have almost no effect on the nighttime concentrations.

To qualify as a large source the convective eddies produced by the city heat flux must be weak enough that the plume rises through the nighttime mixing layer into the stable layer above. This condition is only satisfied in Boston at night when $L < L^*$.

The plume rise in the stable region above the mixing layer must be sufficient to bring the bottom of the plume above the mixing layer. This will occur when the inequality in Eq.(8) is satisfied. In Boston the nighttime mixing depth, L , is estimated to be 100 meters (see page 30). Plume rise observations have established a mean value of $\beta = 0.6$ (Refs. 4,5,6). If the value for $\Delta z'_{\max}$, Eq(7) is substituted into Eq.(8) along with the values given above for β and L the following inequality is reached for Boston.

$$h_g + 2/3 \Delta h > 100 \quad \text{Eq.(17)}$$

Sources in Boston which satisfy Eq.(17) are considered large sources. This definition only applies inside the core area where a well defined mixing layer exists. The large sources in the core area of Boston are listed

according to size in Table 7. Their location in the core area is indicated in Fig.(9).

The relative frequency of large sources in metropolitan Boston is indicated in Fig.(8). The volume flow rate, CFM, is used as the simplest measure of source size. Of the 419 point sources in metropolitan Boston (Refs. 19 and 20), only 35 satisfy the conditions in Eq.(17).

Table 7

Source	h_s (meters)	CFM per stack (thousands)	$h_s + 2/3 \Delta h$
1. Boston Edison (Mystic)	103	400	205
2. Boston Edison (Summer St.)	76	400	180
3. Boston Edison (Summer St.)	81	250	170
4. Boston Edison (Mystic)	79	250	170
5. Boston Navy Yard	54	208	135
6. Boston Edison (Kneeland St.)	79	180	155
7. MBTA (First St.)	34	150	160
8. MBTA (Lincoln St.)	76	150	150
9. Cambridge Electric (Blackstone St.)	47	150	120
10. Cambridge Electric (First St.)	54	140	125
11. Gillette	49	106	115
12. M.I.T.	53	100	120
13. Boston University	30	75	105
14. Revere Sugar	44	60	105
15. Harvard Medical School	49	55	100
16. Penn Central R.R.	61	54	120
17. Chelsea Naval Hospital	44	53	105
18. Mass. Soldiers Home	46	49	105
19. Boston City Hospital	76	38	125
20. Boston Engine Terminal	61	36	105
21. Statler Hilton	55	28	100
22. New England Confectionery	61	20	105

Line Source Model

The assumptions made in this model are similar to those in previous models. The goal is to obtain the simplest model which will help to explain the diurnal differences in the diffusion process for urban areas. The assumption is that pollutants which reach equilibrium in the mixing layer are uniformly distributed throughout it. Plume aerodynamics allows the fraction of the total source strength which is trapped in the mixing layer to be calculated.

In the manner of Holzworth (Refs. 33, 35) the primary variables affecting the concentration in the mixing layer are assumed to be mixing depth, wind speed, and source strength. Plume aerodynamics, as discussed earlier, suggests that during the majority of the daylight hours all pollutants are trapped in the mixing layer, while at night only half of the pollutants released from small sources are trapped in the mixing layer. These assumptions lead to two equations; one describes the average daytime concentrations, and the other describes the average nighttime concentrations in an urban area.

$$C = K \frac{\Gamma_t}{VL} \quad \text{Eq.(18)}$$

$$C = K \frac{\frac{1}{2} \Gamma_s}{VL} \quad \text{Eq.(19)}$$

The area modeled is the section of metropolitan Boston shown in Fig. 9 with each side having a length of ten kilometers. The results of Fay and Flowers (Ref. 36) indicate that the concentrations produced by all the upwind sources will dominate the effect of nearby sources for a city of this size. According to Holzworth (Ref. 33) the travel time required for a

plume to cross the city is long enough that the plumes which are trapped in the mixing layer will be uniformly distributed throughout it. This is further supported by the helicopter soundings in New York reported by Davidson (Ref. 14). Sources outside the area modeled were ignored. The justification for this simplification is that approximately 3/4 of the annual SO₂ emissions for metropolitan Boston occur in the area modeled; while it only comprises 1/7 of the total land area. The final correlation obtained is probably as good as it is because the added SO₂ flux from sources upwind of the area modeled helps to compensate for the SO₂ flux loss from sources at the downwind edge of the area modeled.

Observed Air Quality

The accuracy of the model is determined by comparing the predicted and observed concentrations. The air quality monitoring stations in the core area are indicated in Fig. (9). At least three and normally four of the monitoring stations were operating at the same time. Concentrations observed during the same time period were averaged together in the manner of Mahoney (Ref. 37) to obtain an estimate of the city wide concentration. Seasonal maximum concentrations were handled in the same way although there is no indication that the observed maximum occurred simultaneously at all stations. The average city concentration calculated in this fashion is listed in Table 8. These seasonal values are plotted against the concentrations predicted by the line source model in Figs. (11-14). There are not enough observations to accurately determine the standard deviation so the error brackets in the figures are the maximum and minimum concentration

observed during the indicated season. The solid diagonal line in the figures has a slope of 1 and indicates the locus of points which would represent a perfect fit between observed and predicted values.

Table 8

(in PPM)	1966	1970	1971	1972
Annual average	.052	.039	.023	.012
Winter average (3 mos.)	.067	.072	.041	.018
Summer average (3 mos.)	.026	.021	.012	.006
24 hr. max. Winter	-	-	.127	.051
Concentration Summer	-	-	.052	.031
1 hour max. Winter	-	-	.261	.163
Concentration Summer	-	-	.183	.130
o/o Sulfur in residual fuel	2.2	2	1	0.5

Estimation of Line Source Strength

SO₂ production from the large sources indicated in Table 7 was obtained from the 1970 point source listing. SO₂ production for the small sources in 1970 was determined from the source listing and the apportioning factors for core area towns (Ref. 20). It is estimated that the 100 sq. kilometer section of the core area shown in Fig. (9) contains: all the utilities, 60% of the point sources (most of these qualify as small sources), 50% of the commercial and industrial area sources, and 30% of the residential sources in the metropolitan Boston area.

Given this division of sources, the SO₂ production for metropolitan Boston in 1966 (Ref. 19) can be apportioned to determine the fraction which was emitted in the area of interest. To determine the SO₂ production for 1971 and 1972, it was assumed that the fuel consumption and operating conditions reported in the 1970 study remained constant. The percent of sulfur in distillate fuel remained about the same so the SO₂ production from sources burning distillate fuel remained constant between 1970 and 1973. In 1970, when the survey of sulfur dioxide emissions in metropolitan Boston was made, the sulfur content of residual fuel was 2% (Ref. 19) in the core area. In October, 1970, the allowable sulfur content in residual oil in the core area was reduced to 1% (Ref. 21). It is assumed that this reduced the annual emission of SO₂ for 1971 by 50%. In October, 1971, the allowable sulfur content in the core area was reduced to 0.5% (Ref. 21) reducing the annual SO₂ emission from residual oil by another 50% during 1972. Table 9 lists the tons of SO₂ emitted per year in the area modeled obtained by making the assumptions above.

Table 9

	1966	1970	1971	1972
Small sources	77	63	34	19.5
Large sources	153	126	63	31.5
Total source strength	230	189	97	51.0

(in thousands of tons of SO₂ emitted per year)

The line source model assumes that the line source strength/meter is equal to the total SO₂ flux divided by the length of the line, in this case ten kilometers. The values of the source strength in Table 6, have been divided by 10⁴ meters and appropriate conversion factors to obtain the annual contribution to the line source strength, Γ , from the large and small sources listed in Table 7.

Table 10

Annual contribution from:	1966	1970	1971	1972
Γ_s (small sources)	.22	.18	.10	.06
Γ_L (large sources)	.45	.36	.18	.09
Γ_t (all sources)	.67	.54	.28	.15

(In grams/meter second)

The large sources (utilities) have a relatively constant load throughout the year. The small sources burn more fuel in the winter because of the space heating load. The best way to determine the seasonal variation in the small source strength is to inventory seasonal fuel consumption. This information is not readily available so the following estimation procedure is employed.

The nighttime concentration is only dependent on the small source strength because the large sources do not mix down to ground level during the night. The seasonal difference in the Boston wind speed (Ref. 25) and mixing depth is small, therefore the difference between the summer and winter nighttime concentration is proportional to the seasonal difference in the small source strength. Table 11 compares monthly nighttime and daytime averages to the

seasonal average concentration. The winter nighttime concentrations are approximately three times as big as the summer nighttime concentrations. It is assumed that the winter small source strength is three times the summer small source strength. This implies that the winter small source strength is $3/2$ of the annual average, Γ_s , and the summer small source strength is $1/2$ of the annual average which is listed in Table 10.

Table 11

	Nighttime Concentrations	Daytime Concentrations	Average
73 winter	.037	.031	.035
73 summer	.010	.010	.011
72 winter	.038	.038	.038
72 summer	.012	.015	.015
71 winter	.071	.073	.072
71 summer	.021	.025	.023

(In PPM)

Weekly and daily variations in source strength have been observed in other cities (Refs. 13,30). These variations have been ignored in this preliminary study. The diurnal variation in the small source strength is the most significant for this type of study. In other cities the nighttime source strength has dropped to half of the daytime strength. More detailed information regarding the nighttime mixing depth and variation of source strength is necessary to improve the estimations in the following sections.

Seasonal Concentrations

The average seasonal daytime and nighttime concentrations can be predicted with Eqs.(18) and (19). The average meteorological conditions and the best estimate of the source strength, in terms of the annual average source strength (Table 10), are listed in Table 12.

Table 12

	L	V	Γ
Annual average (day)	850	5.75	$\Gamma_L + \Gamma_s$
(night)	100	5.75	Γ_s
Winter average (day)	700	6.4	$\Gamma_L + 3/2 \Gamma_s$
(night)	100	6.4	$3/2 \Gamma_s$
Summer average (day)	1000	5.25	$\Gamma_L + \Gamma_s$
(night)	100	5.25	$1/2 \Gamma_s$

The predicted daytime and nighttime concentrations should be compared with the concentrations observed during the same time period. Unfortunately, the only data available in hard copy for 1966 and 1970 are the seasonal twenty-four hour average concentrations (Ref. 18). Table 11 indicates that the daytime, nighttime, and 24 hour monthly average are nearly the same. The same pattern was found by Mahoney (Ref. 37) in 1966. This is a coincidence resulting from the distribution of small and large sources in Boston, Fig.(8), and the diurnal variation in the mixing depth.

In Figs. (11) and (12) the annual and seasonal daytime and nighttime concentrations predicted by the line source model are compared with the

average 24 hour concentration. The daytime concentrations predicted by the line source model, Eq.(18), Fig. (11), are in very good agreement with the observed concentrations. The predicted nighttime concentrations, Eq.(19), Fig.(12), are 30% to 40% higher than the observed concentrations. This is probably due to the decrease in the small source strength at night which has been neglected.

Figs.(11) and (12) indicate that this simple line source model using two meteorological variables, L and V, predicts concentrations which are historically consistent with the concentrations observed in the core area of Boston over the last eight years. The small source strength is more than sufficient to predict the nighttime concentrations. Therefore, the hypothesis that large sources do not mix down into the mixing layer at night is consistent with our physical understanding of plume rise and the nighttime concentrations observed in Boston.

This model can be used to predict the effect on the environment if large sources are allowed to burn 2% sulfur fuel while the small sources remain at the current 0.5% sulfur level. The small source strength would remain the same, $\Gamma_s = .06$, but the large source strength would return to the 1970 level, $\Gamma_L = .36$, (Table 10).

The annual nighttime concentrations would not be affected if large sources burn high sulfur because the small source strength stays constant. The annual daytime concentration is calculated with the average annual mixing depth and wind speed (Table 12) but the annual daytime source strength is $\Gamma_t = \Gamma_s + \Gamma_L = .42$. Eq.(13) gives an annual daytime concentration of $C = .030$ PPM. This daytime annual concentration combined with the current

annual nighttime concentration, $C = .010$ PPM , will produce an annual concentration of $.020$ PPM .

Twenty-Four Hour Maximum Concentrations

Maximum concentrations result during extreme meteorological conditions. Figs.(1-6) indicate the range of conditions which are likely to occur in Boston. Accurate prediction of short term (daily or hourly) concentrations requires a detailed source and meteorological inventory. An estimate can be obtained by assuming the worst meteorological conditions in terms of air pollution and calculating the concentrations which these conditions would produce. Short term concentrations predicted in this manner will be less accurate than annual or monthly predictions.

Maximum 24 hour concentrations are normally associated with stagnating anticyclones (subsidence inversion). Although the mixing depth is frequently lower than normal during a subsidence inversion, the low wind speeds which generally accompany subsidence inversions are the primary cause of high 24 hour average concentrations. During a subsidence inversion low wind speeds sometimes persist for four or five days (Ref. 38).

Table 2 and Fig.(7) indicate that the lowest wind speed which occurs with any frequency in Boston is $V = 2$ meters/sec. At night the low wind speed and haze which accompany a subsidence inversion encourage the formation of a mixing layer. The minimum nighttime mixing depth during a subsidence inversion is assumed to be 100 meters. During the day the mixing layer cannot break through the base of the subsidence inversion. The minimum daytime mixing depth (base of the subsidence inversion) is assumed to be 500 meters.

Table 13 lists the conditions to be used with Eqs.(18) and (19) to estimate the maximum daytime and nighttime concentrations.

Table 13				
	Winter		Summer	
	Day	Night	Day	Night
V (meters/sec)	2	2	2	2
L (meters)	500	100	500	100
Γ	$3/2 \Gamma_s + \Gamma_L$	$3/2 \Gamma_s$	$1/2 \Gamma_s + \Gamma_L$	$1/2 \Gamma_s$

The daytime and nighttime conditions listed in Table 13 are assumed to occur during the same 24 hour period in order to produce the 24 hour maximum concentration. The 24 hour concentration is the average of the daytime and nighttime concentration weighted by the number of hours of daylight.

$$\text{24 hour concentration} = \frac{\left(\begin{array}{c} \text{daytime} \\ \text{concentration} \end{array} \right) \left(\begin{array}{c} \text{hours of} \\ \text{daylight} \end{array} \right) + \left(\begin{array}{c} \text{nighttime} \\ \text{concentration} \end{array} \right) \left(\begin{array}{c} \text{hours of} \\ \text{darkness} \end{array} \right)}{24 \text{ hours}}$$

(Eq. 20)

Fig. (13) compares the predicted and observed seasonal variation for the 24 hour maximum concentration. The meteorological assumptions listed in Table (13) overestimate the maximum concentration by about 15%. Historically the highest 24 hour concentrations have occurred during the winter months because the space heating load increases the daytime and nighttime source strength. During the winter months it is dark 2/3 of the time so the nighttime concentration is the major cause of high 24 hour maximum concentrations. In the past the small sources which produce the nighttime concentrations have been the principal cause of high 24 hour averages during the winter

months while large sources contribute more during the summer months.

The conditions listed in Table 13 can be used to estimate the 24 hour maximum concentrations which will be produced if large sources are allowed to burn 2% sulfur fuel all the time. The small source strength, stays at its current level, $\Gamma_s = .06$. The large source strength increases to $\Gamma_L = .36$. This causes the daytime source strength to be five times the nighttime source strength during the winter, where as in the past it has only been twice as large. The result is that the daytime contribution to the 24 hour maximum concentration is about the same as the nighttime contribution during the winter and much larger during the summer.

Table 14 lists the seasonal 24 hour maximum concentrations which are expected if large sources burn high sulfur fuel all the time. The seasonal difference is small because the daytime concentration is the dominant effect and does not change much from summer to winter.

Table 14

	Winter	Summer
24 hour maximum concentration (PPM)	.105	.100

One Hour Maximum Concentrations

One hour concentrations are calculated by adding the background concentration in an urban area to the local contributions from individual sources, (Eq.(21)). One hour maximum concentrations generally occur during the day when the large sources, which produce the highest contributions to ground level concentrations, mix down to ground level. The highest one hour concentrations are observed directly beneath the plumes from these large sources. There is a lot of scatter in observational data for one hour maximum concentrations because the plumes from the large sources are rarely above the monitoring stations during the worst meteorological conditions.

$$\begin{array}{l} \text{One hour} \\ \text{concentration} \end{array} = \begin{array}{l} \text{Background} \\ \text{concentration} \end{array} + \begin{array}{l} \text{Local contribution} \\ \text{from an individual} \\ \text{source} \end{array} \quad \text{Eq.(21)}$$

$$\begin{array}{l} \text{Maximum local contribution} \\ \text{from an individual source} \\ \text{with a one hour sampling} \\ \text{period} \end{array} \quad C_i \text{ (PPM)} = K \frac{\Gamma_i}{10V h_e^2} \quad \text{Eq.(22)}$$

The maximum contribution from an individual source is estimated with the diffusion Eq.(22), (Refs. 7,29). The effective stack height, h_e , is the plume equilibrium position and changes during the day depending on the meteorological conditions. The background concentration is estimated with the line source model, Eq.(18). Since both the background concentration and the contribution from an individual source increase with decreasing wind speed, the one hour maximum concentration is estimated with the lowest wind speed frequently observed in Boston, $V = 2$ meters/sec.

High one hour concentrations are frequently observed in the early morning and just after noon. In the early morning the background concentration is high because the mixing layer is low. At noon the contributions from the individual sources are high due to the low effective stack heights caused by strong convective turbulence.

The highest background concentration in the early morning occurs when the emissions from all the large sources are trapped in the mixing layer. This is assumed to occur when the mixing depth reaches 300 meters. The highest contribution from an individual source at this time occurs when the pollutants which are emitted from a large source during the night are mixed down to ground level (fumigation). The lowest early morning effective stack height (nighttime equilibrium position of the plume) occurs when there is no nighttime mixing layer and the atmosphere is stable at ground level. The minimum effective stack height with low wind speed is estimated with Eqs.(14) and (16) using $\frac{d\theta}{dz} = 5 \times 10^{-3} \text{ }^{\circ}\text{C/M}$. The maximum contribution from a large source in the morning is calculated with this effective stack height and Eq.(22).

The strongest convective turbulence occurs when the mixing layer and solar heat flux are at their maximum values. The maximum seasonal solar heat flux, I_0 (Figs. 1 and 2), which occurs less than 25% of the time is used to estimate Q_r at noon, Eq.(10). The maximum mixing depth is estimated with Eq.(1) using the maximum observed solar heat flux minimum lapse rate, Fig.(3), because the data base for the observed mixing depth is very small. The maximum one hour contribution from a large source at noon is estimated with these meteorological conditions and Eqs.(13,14 and 22) (Table 15).

Table 15 lists the meteorological conditions used to estimate the maximum one hour concentration in the early morning and at noon. The average one hour concentration is estimated using the average meteorological conditions, Tables 1 and 12.

Table 15

	V (meters/sec)	L (meters)	Q_r (cal/cm ² sec)	$\frac{d\theta}{dz}$ (°C/meters)
Early Morning	2	300	-	5×10^{-3}
Noon: Winter	2	1100	.72	2.5×10^{-3}
Summer	2	2000	1.4	2.5×10^{-3}

The individual contributions to ground level concentrations were estimated for the largest 35 sources in metropolitan Boston. The large sources in the core area produce the highest contributions. Different sources produce the highest contribution during different meteorological conditions. Table 16 lists the highest contribution expected from any of the large sources in the core area when they are burning 2% sulfur fuel. Due to the uncertainty in this sort of calculation, the sources which are expected to produce concentrations within 25% of the maximum contribution are also listed. To obtain the highest contribution in 1971 (1% sulfur fuel) or 1972 (0.5% sulfur fuel) the values listed in Table 16 are divided by the appropriate factor.

Table 16

Time of Day	Early Morning	Noon Winter	Noon Summer
Maximum contribution to ground level concentrations (In PPM)	.088	.26	.41
Sources with contributions within 25% of the maximum	5,9-14	5,9-13	1-5,9-13

The maximum one hour concentrations were estimated for 1% sulfur fuel (1971) and 0.5% sulfur fuel (1972 and 1973). During the winter the early morning concentration is 30% greater than the noon concentration. This is because the source strength is high and the turbulence is low in the winter. During the summer the situation is reversed and the noon concentration is 20% greater than the early morning concentration. Fig.(14) compares the highest predicted seasonal one hour concentration with the highest observed concentrations.

Historically all sources have burned residual fuel with the same sulfur content. As this model predicts, in the past the maximum one hour concentrations have occurred in the winter. If only large sources burn high sulfur fuel this pattern is expected to change. The same estimation procedure is used, but the large source strength returns to its 1970 level, Tables 10 and 16. In this case the one hour maximum concentration is expected at noon during the summer. Table 17 lists the maximum one hour concentrations predicted in the early morning and at noon if large sources burn high sulfur fuel.

Table 17

	Early Morning	Noon
Winter	.36	.33
Summer	.31	.45

(In PPM)

Fuel Switching to Meet the Standards

If unrestricted burning of high sulfur fuel by large sources is allowed during the summer or winter, the predictions of maximum ground level concentrations on the preceding pages suggest that the current air quality standards will be exceeded. Table 18 summarizes the predictions and the existing standards. The concentrations predicted for average conditions represent the fiftieth percentile of the cumulative frequency distribution for predicted concentrations. Fifty percent of the time the concentrations are expected to be less than the average value. The concentrations predicted for extreme conditions are representative of the maximum concentrations likely to be observed; they are expected to occur infrequently.

Table 18

	Annual average concentration	Season	24 hour max concentration	1 hour max concentration
Extreme conditions		Winter	.105	.36
		Summer	.100	.45
Average conditions	.020	Winter	.043	.150
		Summer	.035	.170
Existing standards	.025		.105	.28

(In PPM)

It is anticipated that the current air quality standards can be met if the large sources burn low sulfur fuel during most of the daylight hours. The frequency distribution of wind speed (Fig.(7), Table 2) is the simplest estimate for the occurrence of extreme meteorological conditions. The amount of time that high sulfur fuel can be burned during the day is estimated by determining what portion of the time the wind speed is high enough to maintain acceptable air quality. To make the estimate more conservative, the maximum allowable ground level concentrations are kept 25% below the existing standards. The predicted air quality then may not exceed the following averages: Annual = .019, 24 Hour = .076, 1 Hour = .21.

First, the calculation is done for the average city wide concentrations, neglecting the upper limit of the error brackets in Figs. (11-14). The annual average is virtually satisfied already, and the fuel switching which is necessary to meet the other two standards will sufficiently reduce the annual average concentration. The one hour maximum concentration is more

difficult to meet than the 24 hour maximum concentration. The concentrations estimated in Table 18 are assumed to be inversely proportional to the wind speed. Using this assumption the minimum wind speed which will satisfy the reduced standards on page 51 can be estimated. During the winter months high sulfur fuel can be burned in the daytime by large sources if the wind speed is above 4 meters/sec. (8 knots). During the summer months high sulfur fuel can be burned in the daytime by large sources if the wind speed is above 4.3 meters/sec. (8.5 knots).

Referring to Table 2 the percentage of daylight hours during which the wind speed is high enough to allow high sulfur fuel to be burned is obtained. Finally it is assumed that it is daylight during 60% of the summer hours and 40% of the winter hours. Combining these percentages, the average city concentrations are expected to be 25% below the existing standards if high sulfur fuel is burned in the following manner:

During the winter 90% of the time.

During the summer 75% of the time.

A second estimate of the percentage of time high sulfur fuel may be burned can be obtained if the highest concentration observed anywhere in the city must be kept 25% below the existing standards. Figs. (11-14) indicate that the line source model underestimates the maximum concentrations observed anywhere in the city by 50%. The minimum wind speed which would maintain adequate air quality is 50% higher when the highest observed concentrations are considered, but the same pattern exists. During the winter the minimum wind speed is 6 meters/sec. (12 knots). During the summer the wind speed is 6.4 meters/sec. (13 knots). These minimum wind speeds reduce

the percentage of time that high sulfur fuel may be burned to:

During the winter 80% of the time.

During the summer 55% of the time.

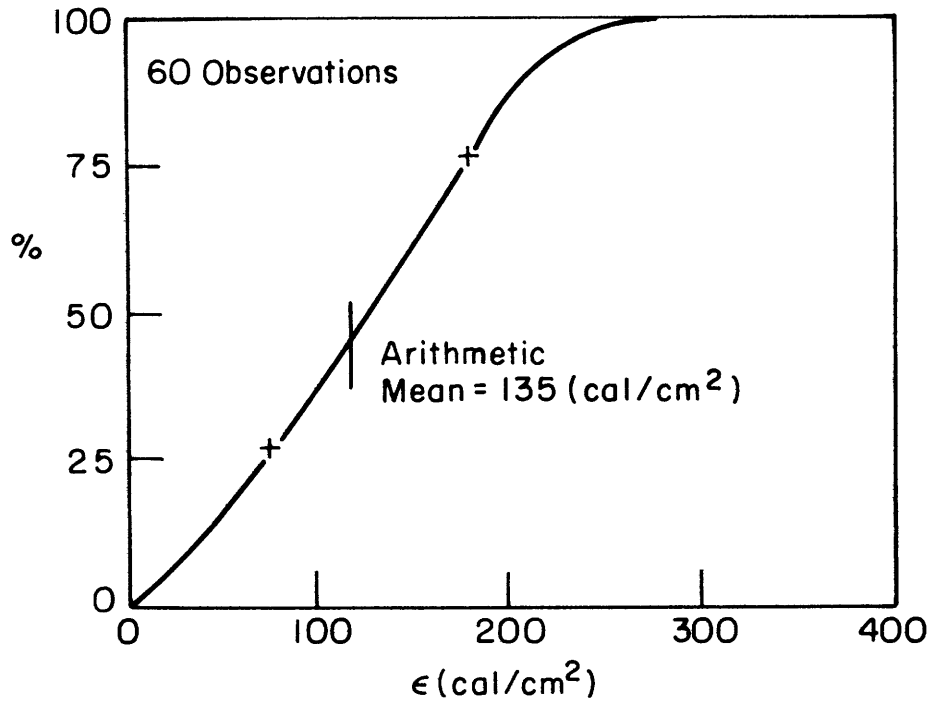


Figure 1 Daily Solar Heat Flux in January
% Less than ϵ

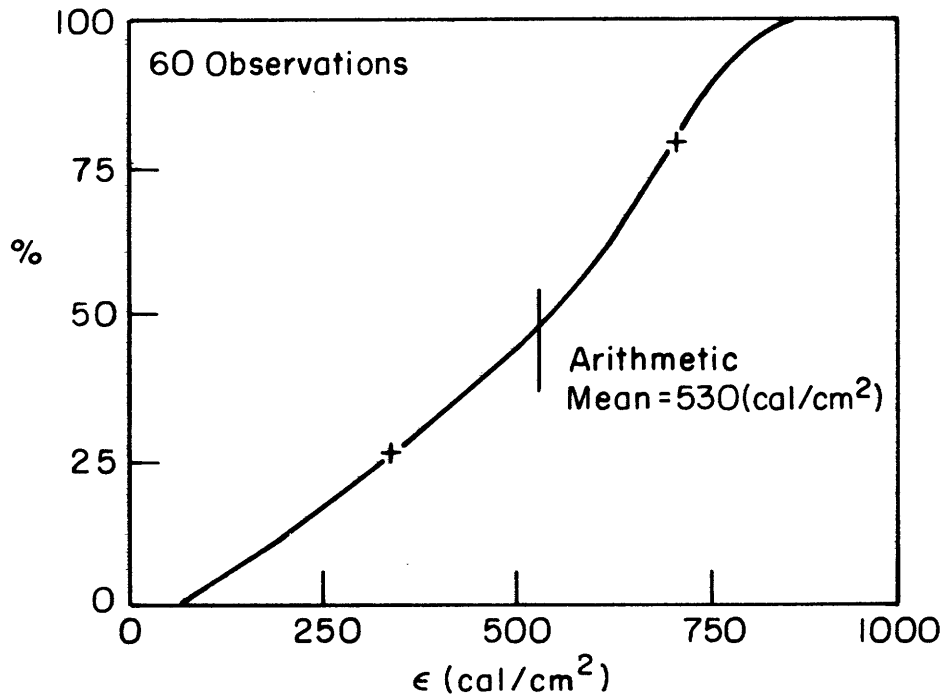


Figure 2 Daily Solar Heat Flux in June
% Less than ϵ

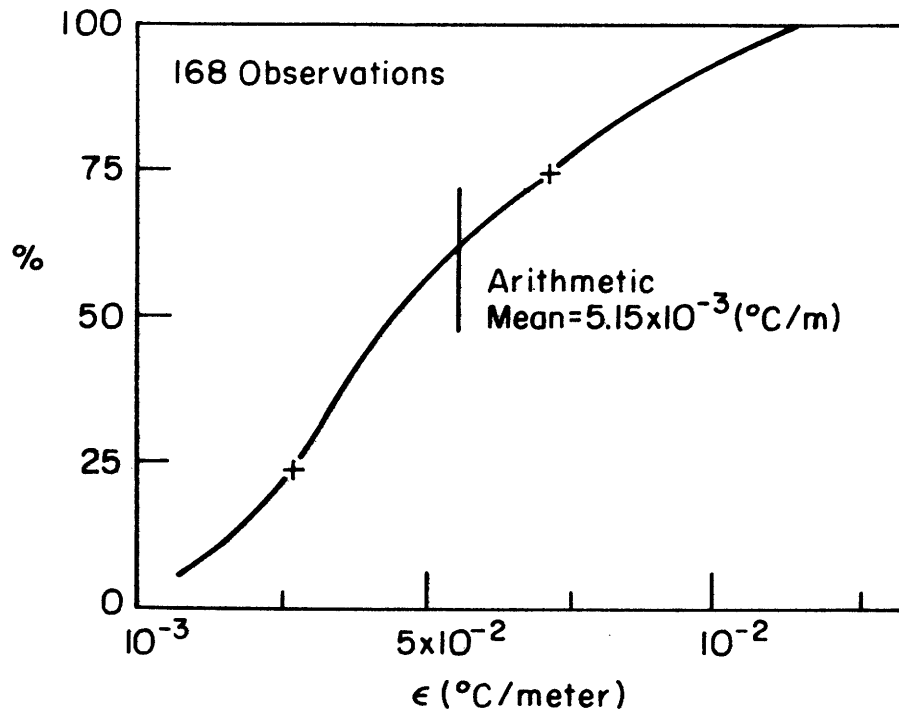


Figure 3 Annual Lapse Rate (Potential Temperature) % Less than ϵ

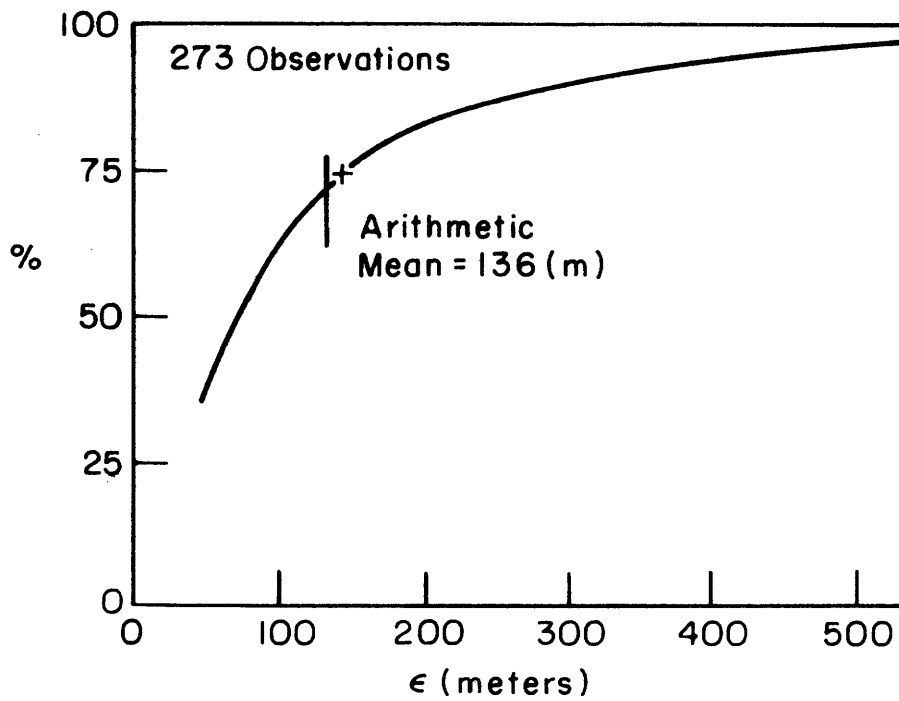


Figure 4 Mixing Depth at 7:00 AM % Less than ϵ

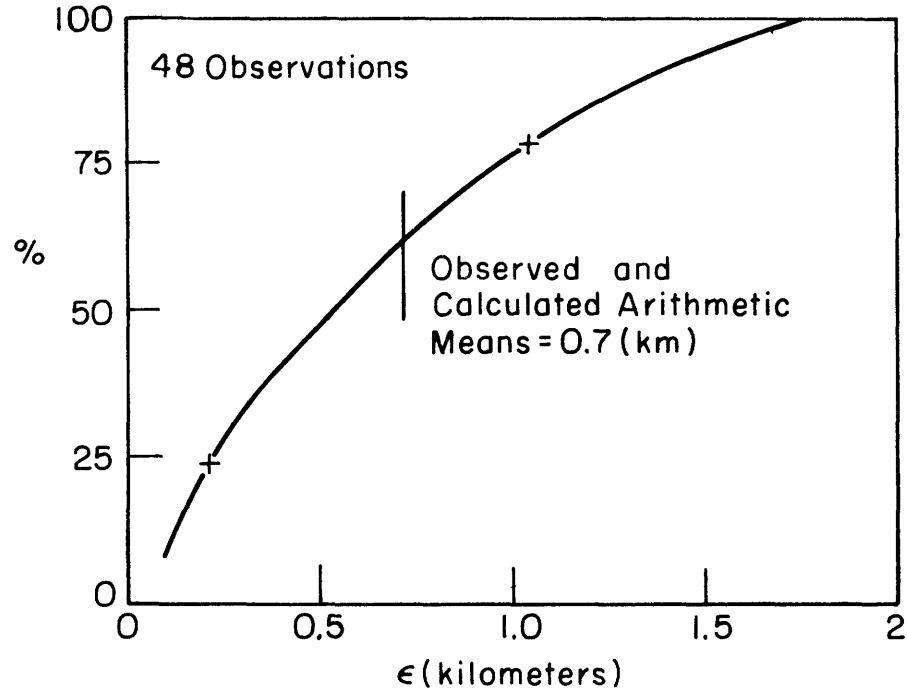


Figure 5 Convective Mixing Depth for Winter Months at Noon % Less than ϵ

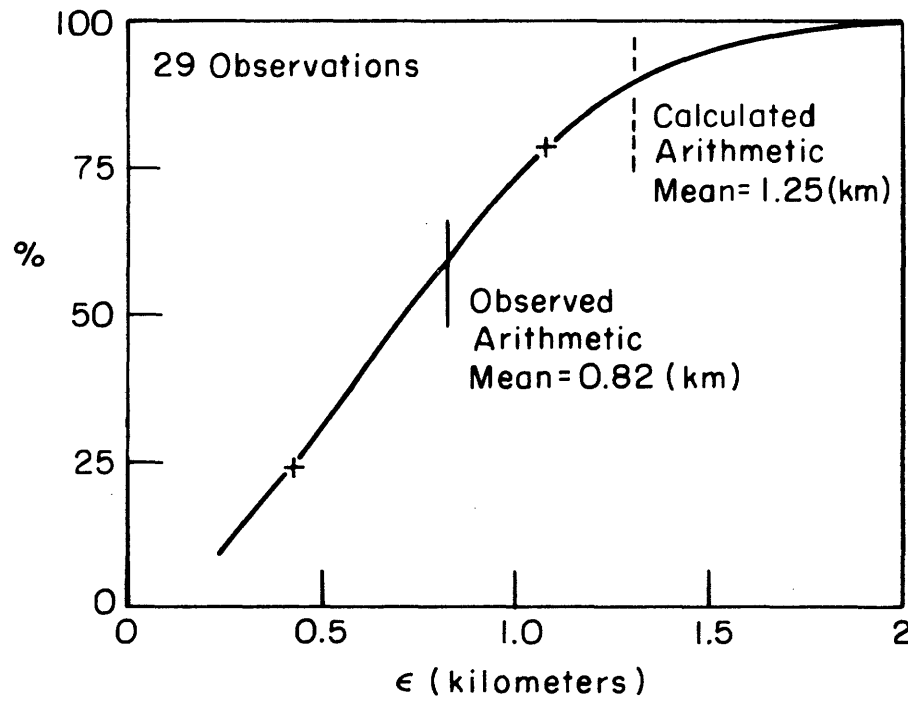


Figure 6 Convective Mixing Depth for Summer Months at Noon % Less than ϵ

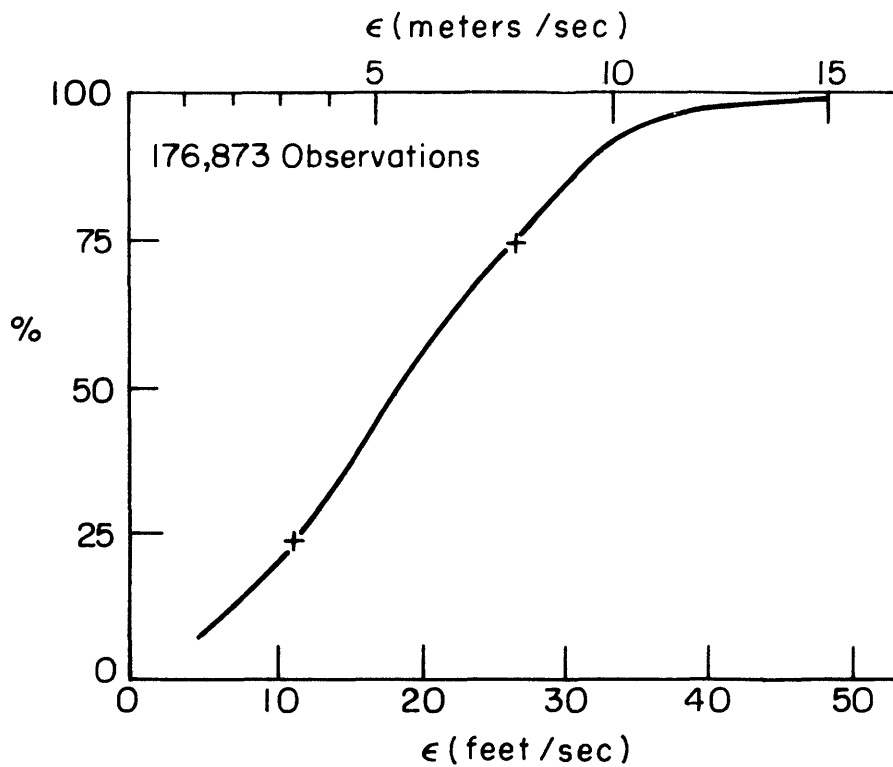


Figure 7 Wind Speed at Logan Airport
% Less than ϵ

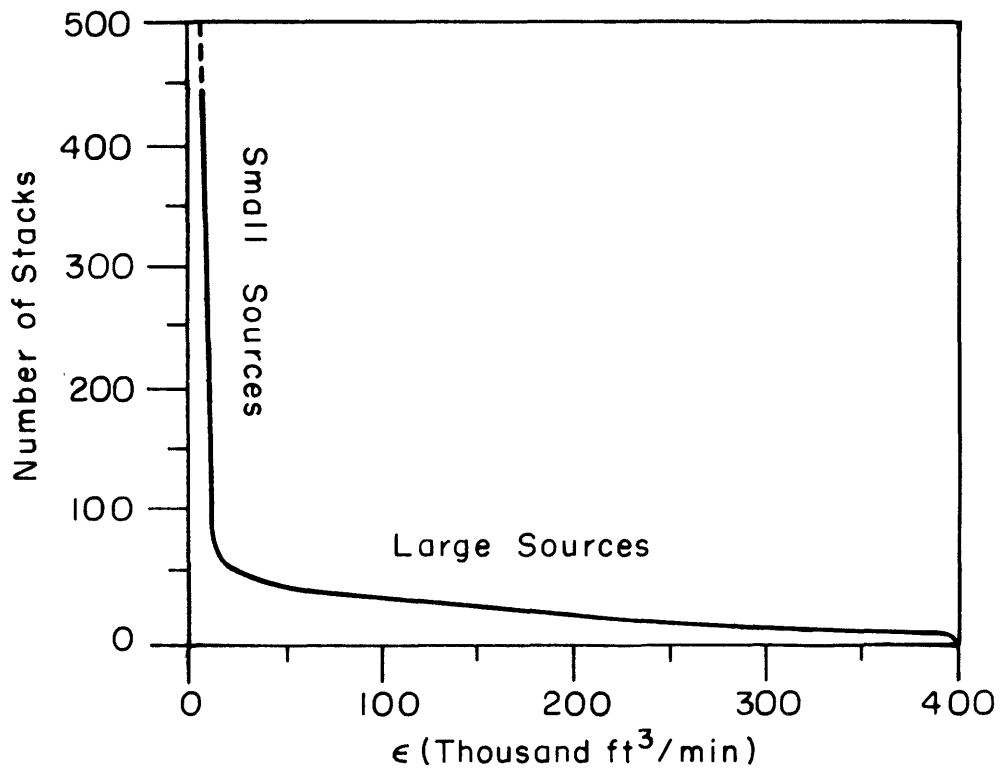
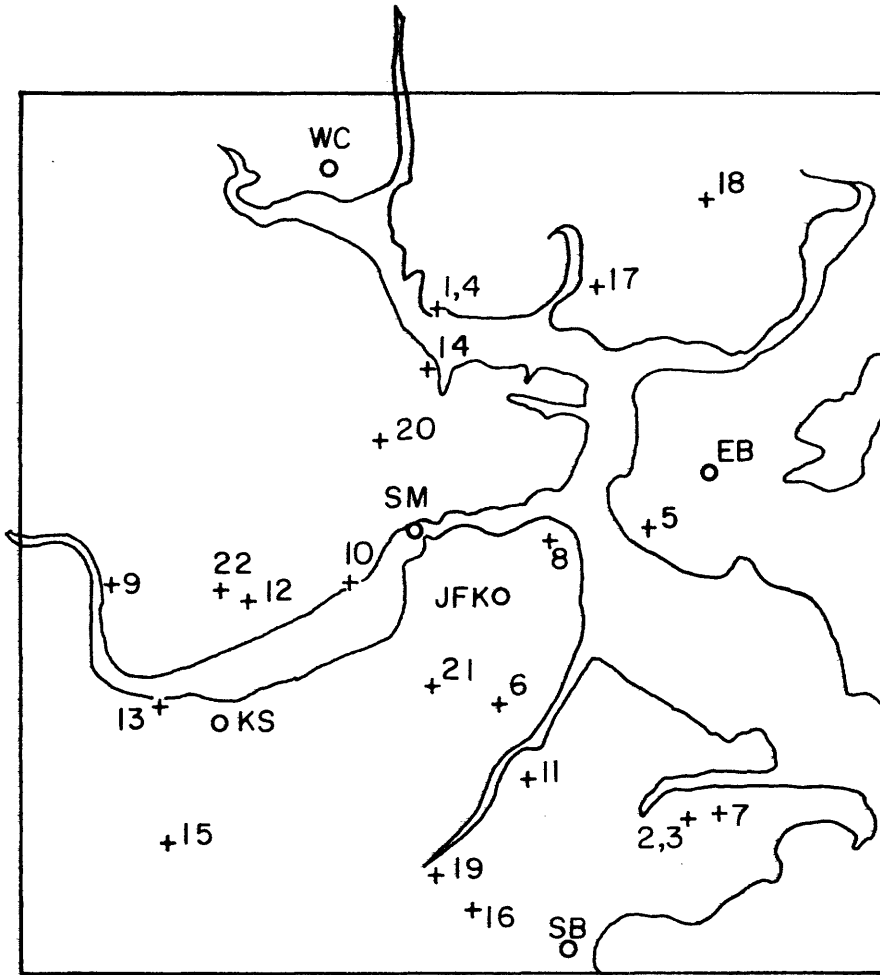
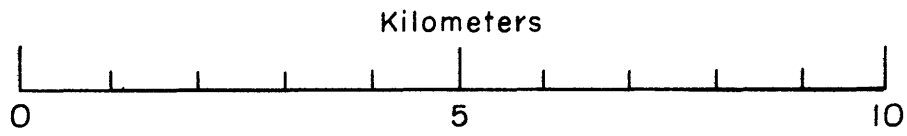


Figure 8 Point Source Size Distribution Number of
Stacks with Volume Flow Rate Less than ϵ



+ Large Point Sources in 100 sq.km. Section
(See Table 7)

o Air Quality Monitoring Sites

- EB East Boston
- JFK John F. Kennedy Building
- KS Kenmore Sq.
- SM Science Museum
- SB South Boston
- WC Wellington Circle

Figure 9 Section of Core Area Modeled

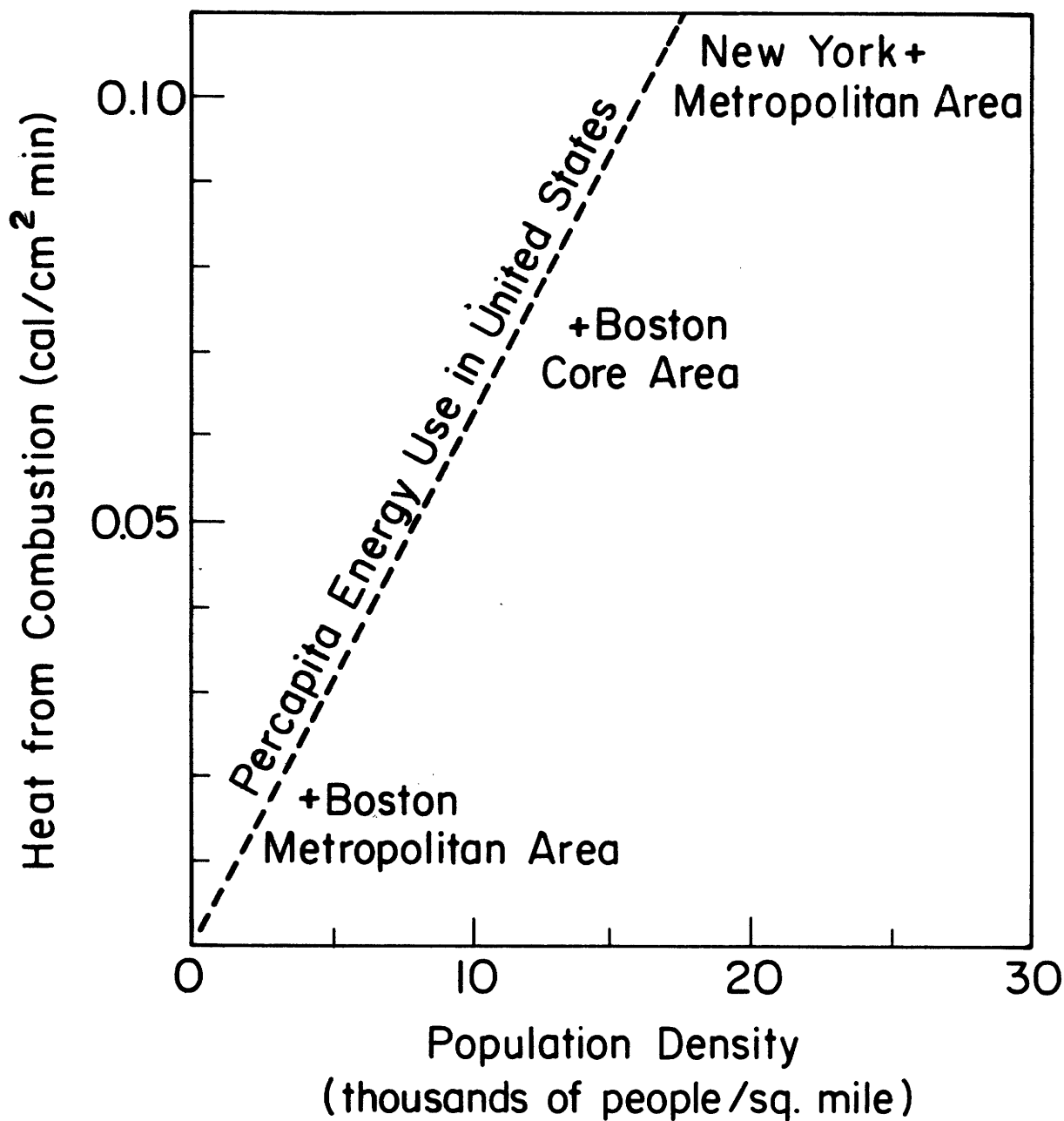


Figure 10 Heat from Combustion vs Population Density

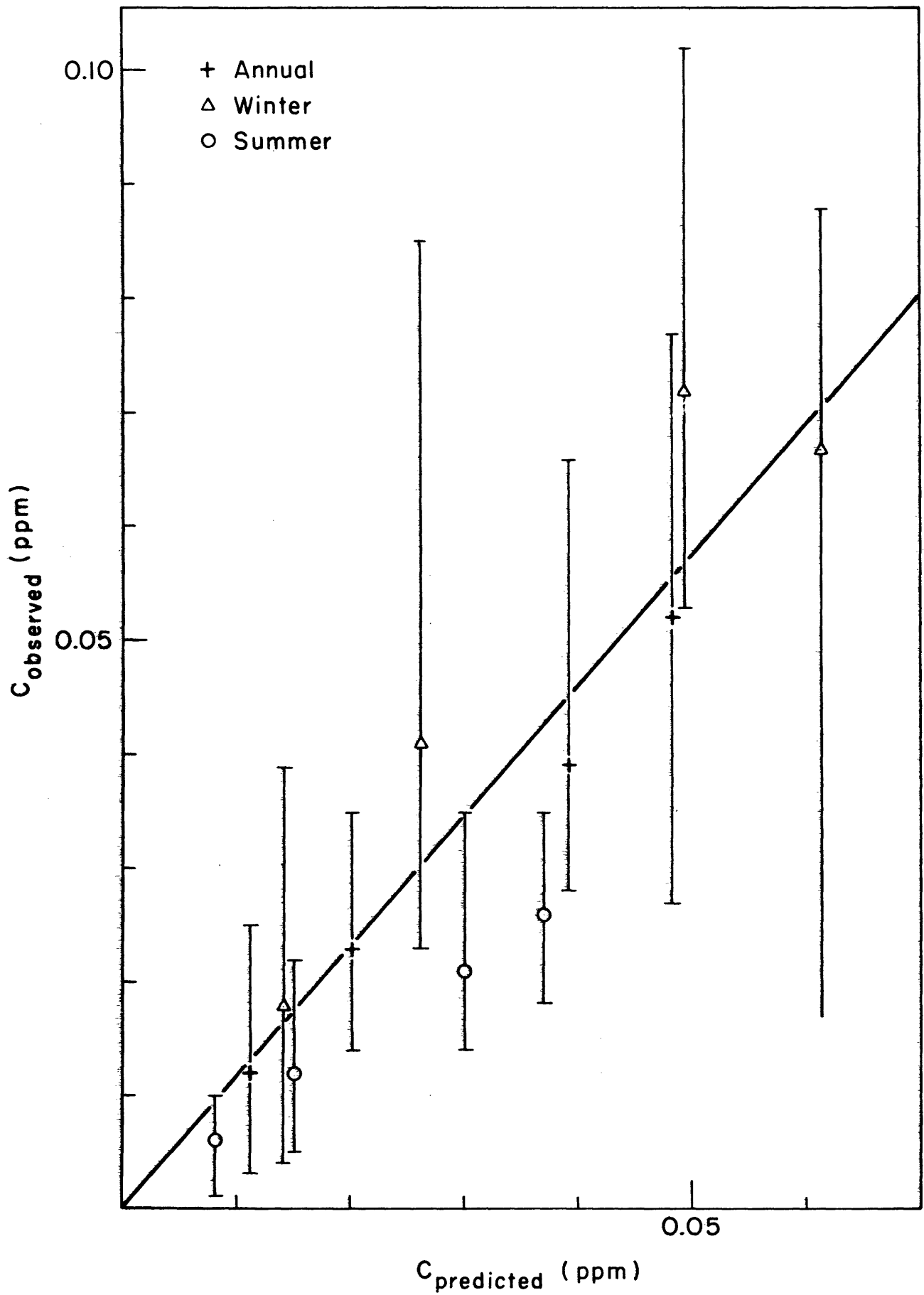


Figure 11 Annual and Seasonal Daytime Concentrations

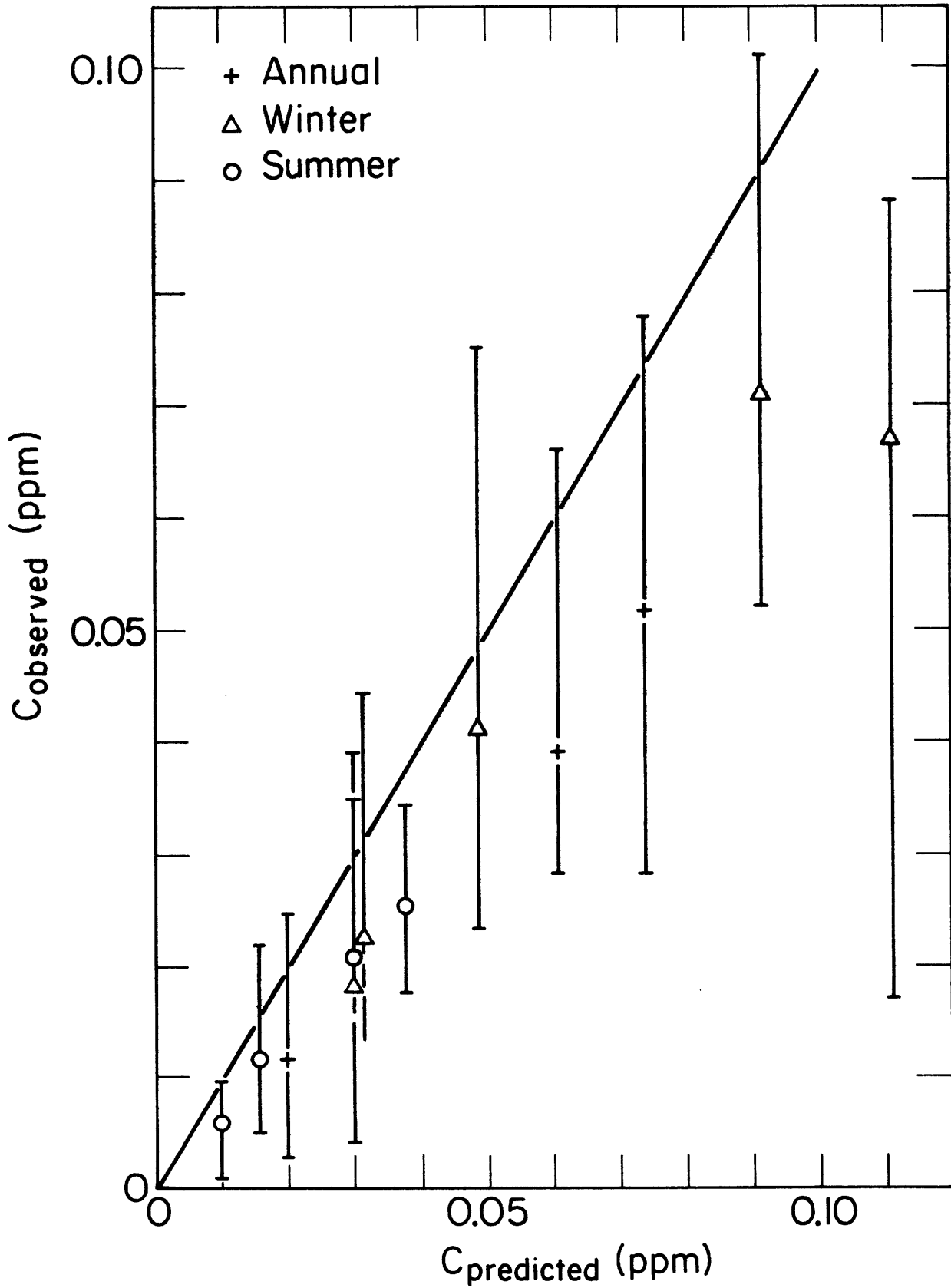


Figure 12 Annual and Seasonal Nighttime Concentrations

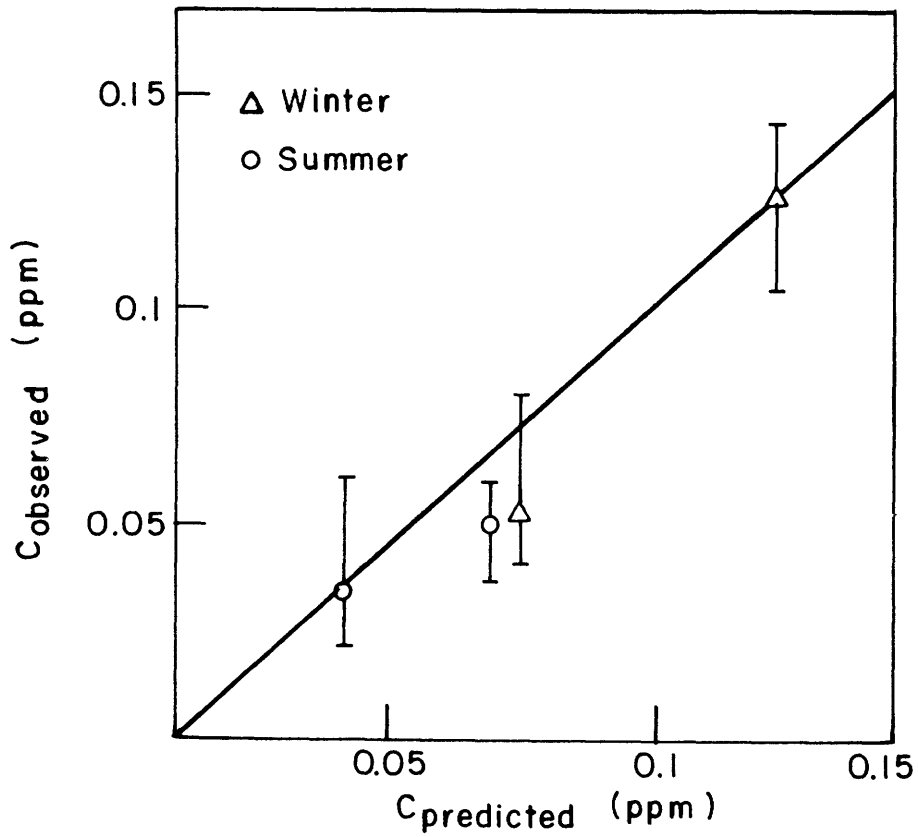


Figure 13 Seasonal 24 Hour Maximum Concentrations

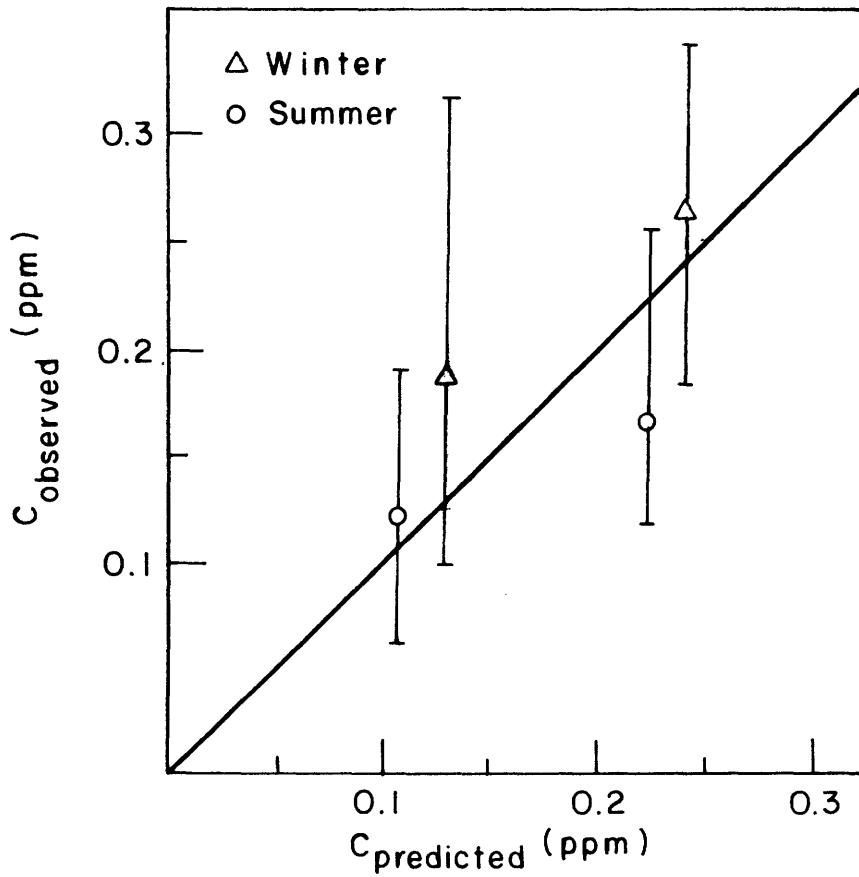


Figure 14 Seasonal 1 Hour Maximum Concentrations

References

1. Mahoney, James R., Project Director, Differential Evaluation of the Massachusetts Stationary Source Air Pollution Control Regulations, Cambridge, Mass., Harvard Univ., School of Public Health, 1973.
2. Roberts, J.J., Croke, E.S., Kennedy, A.S., "An Urban Dispersion Model", Proceedings of Symposium on Multiple Source Diffusion Models, Stern, A.C., ed., Research Triangle Park, North Carolina, Environmental Protection Agency, 1970.
3. Fay, J.A., "Buoyant Plumes and Wakes", Annual Review of Fluid Mechanics, Van Dyke, M., Vincenti, W.G., Wehamsen, J.V., eds., Palo Alto, Calif., Annual Review Inc., 1973.
4. Hoult, D.P., Fay, J.A., Forney, L.J., "A Theory of Plume Rise Compared with Field Observations", Journal of the Air Pollution Control Assn., 19, pp. 535-590, 1969.
5. Fay, J.A., Escudier, M., Hoult, D.P., "A Correlation of Field Observations of Plume Rise", Journal of the Air Pollution Control Assn., 20(6), pp. 391-397, 1970.
6. Hoult, D.P. and Weil, J.C., "Turbulent Plume in a Laminar Cross Flow", Atmospheric Environment, 6, pp. 513-531, 1972.
7. Weil, J.C., and Hoult, D.P., "A Correlation of Ground-Level Concentrations of Sulfur Dioxide Downwind of the Keystone Stacks", Atmospheric Environment, 7, pp. 707-721, 1973.
8. Lumley, J.L., and Panofsky, H.A., The Structure of Atmospheric Turbulence, New York, Interscience, 1964.
9. Chuang, H., Cermak, J.E., "Similarity of Thermally Stratified Flows in the Laboratory and Atmosphere", The Physics of Fluids Supplement, pp. 5255-5262, 1967.
10. Monin, A.S., and Obukhov, A.M., "Basic Laws of Turbulent Mixing in the Ground Layer of the Atmosphere", translated from Akademiia Nauk SSSR, Leningrad, Geofizicheskii Institut, Trudy, 151(24), pp. 163-187, 1964.
11. Peterson, J.T., The Climate of Cities: A Survey of Recent Literature, Raleigh, North Carolina, National Air Pollution Control Administration, 1969.
12. Duckworth, F.S., and Sandberg, J.S., "The Effect of Cities Upon Horizontal and Vertical Temperature Gradients", Bull. Amer. Meteor. Soc., 35, p. 198, 1969.

13. Summer, P.W., "The Seasonal, Weekly, and Daily Cycles of Atmospheric Smoke Content in Central Montreal", Journal of the Air Pollution Control Assn., 16(8), pp. 432-438, 1966.
14. Davidson, B., "A Summary of the New York Urban Air Pollution Dynamics Program", Journal of the Air Pollution Control Assn., 17(3), pp. 154-158, 1967.
15. Bornstein, R.D., "Observations of the Urban Heat Island Effect in New York City", Journal of Applied Meteorology, 17, pp. 575-582, 1968.
16. Clark, J.F., "Nocturnal Urban Boundary Layer Over Cincinnati, Ohio", Monthly Weather Review.
17. Radiosonde Balloon Ascents in Boston Plotted on Adiabatic Charts (EMSU), MIT Meteorology Department, Rm. 54-162, Cambridge, Mass., 1970-1973.
18. Hourly Concentrations from Monitoring Sites in Boston, Mass., Dept. of Public Health, Boston, Mass., 1970-73.
19. Morgenstern, P., Parks, T.R., Calcagni, J., Air Pollutant Emission Inventory for the Metropolitan Boston Control District, Walden Research Corp., Boston, Mass., June, 1970.
20. Point Source Listing and Air Pollution Emission Apportioning Factors For Metropolitan Boston, Mass., Dept. of Public Health, Boston, Mass., 1970.
21. Regulations for the Control of Air Pollution in the Metropolitan Air Pollution Control District, Dept. of Public Health, Bureau of Air Use Management, Boston, Mass., 1970.
22. Trewartha, G., An Introduction to Climate, New York, McGraw-Hill, 1968.
23. Tsang, G., "Concentration of Effluents in a Plume as Predicted by a Model and Observed in the Field", Atmospheric Environment, 4, pp. 545-556, 1970.
24. Daily Solar Radiation Totals for Blue Hills Observatory, National Oceanic and Atmospheric Administration, Environmental Data Service, Asheville, North Carolina, 1971 and 1972.
25. Uniform Summary of Surface Weather Observations, Surface Winds at Logan International Airport, National Oceanic and Atmospheric Administration, Environmental Data Service, Asheville, North Carolina, 1945-65.
26. Sellers, W.D., Physical Climatology, Chicago, University of Chicago Press, 1965.

27. Davies, J.A., "A Note on the Relationship Between Net Radiation and Solar Radiation", Quarterly Journal of the Royal Meteorological Society, 93, pp. 109-115, 1967.
28. Rider, N.E., Robinson, G.D., "A Study of the Transfer of Heat and Water Vapor Above a Surface of Short Grass", Quarterly Journal of the Royal Meteorological Society, 77, pp. 375-401, 1951.
29. Kratzer, P.A., Das Stadtklima (English translation available from ASTIA #AD 284776), Braunschweig, Friedrich View and Sohn, 1956.
30. Harris, N.D., Huffman, J.R., Weiland, J.H., "Another Look at New York City's Air Pollution Problem", Journal of the Air Pollution Control Assn., 18(6), pp. 406-410, 1968.
31. U.S. Bureau of Census, Statistical Abstract of the United States, 93 ed., Washington, D.C., 1972.
32. Kranz, W.T., and Hout, D.P., Design Manual for Tall Stacks, M.I.T. Fluid Dynamics Laboratory, Publication No. 73-3, 1973.
33. Holzworth, G.C., Mixing Heights, Wind Speeds, and Potential for Urban Air Pollution Throughout the Contiguous United States, Research Triangle Park, North Carolina, Environmental Protection Agency, AP-101, 1972.
34. Hosler, C.R., "Low-Level Inversion Frequency in the Contiguous United States", U.S. Monthly Weather Review, 89(9), pp. 319-339, 1961.
35. Miller, E., Holzworth, G.C., "An Atmospheric Diffusion Model for Metropolitan Areas", Journal of the Air Pollution Control Assn., 17(1), pp. 46-50, 1967.
36. Fay, J.A., Flower, W.L., "A Generalized Model of Urban Pollutant Distribution", American Institute of Aeronautics and Astronautics, AIAA paper no. 72-647, New York, June, 1972.
37. Mahoney, J.R., Maddaus, W.O., and Goodrich, J.C., "Analysis of Multiple-Station Urban Air Sampling Data", Proceedings of Symposium on Multiple Source Diffusion Models, Stern, A.C., ed., Research Triangle Park, North Carolina, Environmental Protecting Agency, 1970.
38. Korshover, J., Climatology of Stagnating Anticyclones East of the Rocky Mountains, Cincinnati, Ohio, National Center for Air Pollution Control, 1967.